

U. A. Glasmacher · W. Bauer · N. Clauer ·  
V. N. Puchkov

## Neoproterozoic metamorphism and deformation at the southeastern margin of the East European Craton, Uralides, Russia

Received: 5 May 2003 / Accepted: 26 June 2004 / Published online: 2 September 2004  
© Springer-Verlag 2004

**Abstract** The eastern margin of the East European Craton (EEC) has a long lasting geological record of Precambrian age. Archaean and Proterozoic strata are exposed in the western fold-and-thrust belt of the Uralides and are known from drill cores and geophysical data below the Palaeozoic cover in the Uralides and its western foredeep. In the southern Uralides, sedimentary, metamorphic and magmatic rocks of Riphean and Vendian age occur in the Bashkirian Mega-anticlinorium (BMA) and the Beloretzk Terrane. In the eastern part of the BMA (Yamantau anticlinorium) and the Beloretzk Terrane, K-Ar ages of the <2- $\mu$ m-size fraction of phyllites (potassic white mica) and slates (illite) give evidence for a complex pre-Uralian metamorphic and deformational history of the Precambrian basement at the southeastern margin of the EEC. Interpretation of the K-Ar ages considered the variation of secondary foliation and the diagenetic to metamorphic grade. In the Yamantau anticlinorium, the greenschist-facies metamorphism of the Mesoproterozoic siliciclastic rocks is of Early Neoproterozoic origin (about 970 Ma) and the S1 cleavage formation of Late Neoproterozoic (about 550 Ma). The second wide-spaced cleavage is of Uralian origin. In the central and western

part of the BMA, the diagenetic to incipient metamorphic grade developed in Late Neoproterozoic time. In post-Uralian time, Proterozoic siliciclastic rocks with a cleavage of Uralian age have not been exhumed to the surface of the BMA. Late Neoproterozoic thrusts and faults within the eastern margin of the EEC are reactivated during the Uralian deformation.

**Keywords** Metamorphism · K-Ar dating · Neoproterozoic · Southern Urals · Eastern margin East European Craton

### Introduction

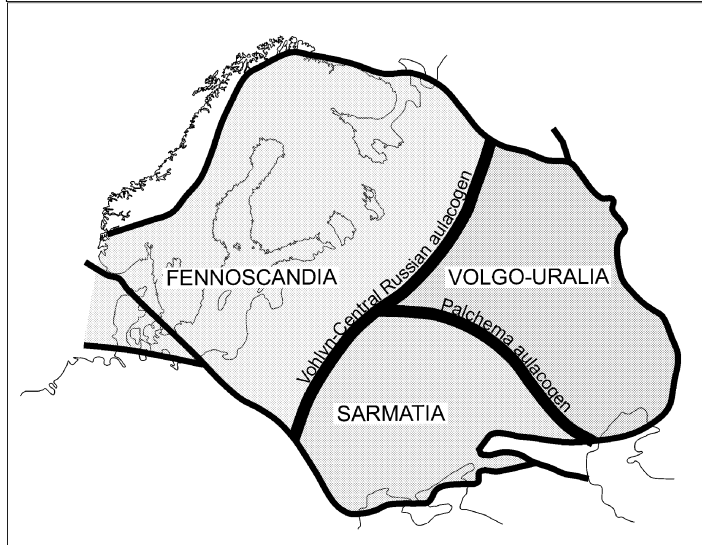
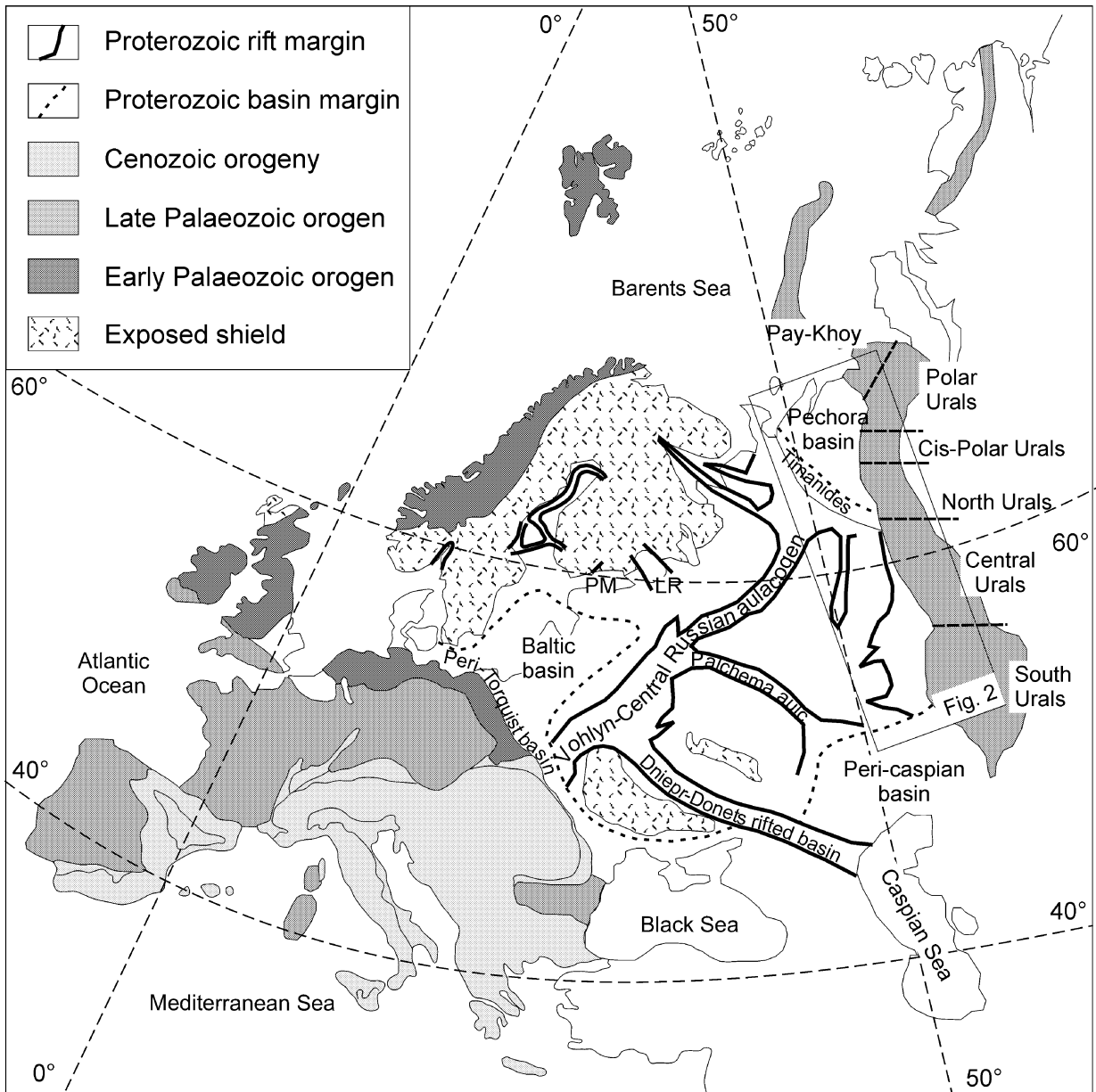
The East European Craton (EEC) consists of the three major Precambrian Terranes: Fennoscandia, Sarmatia and Volgo-Uralia (Fig. 1, Gee and Zeyen 1996; Gorbatschev and Bogdanova 1993). It is bounded to the north by the North Atlantic Margin and to the northwest, the southeast and the south by Phanerozoic orogens. The eastern margin of the EEC has a long lasting Precambrian geological evolution. Crystalline complexes (granulite to amphibolite facies rocks) of Archaean and Palaeoproterozoic age, as well as partly deformed and metamorphosed Meso- and Neoproterozoic strata are exposed in the western fold-and-thrust belt of the Uralides and are known from drill cores and geophysical data below the Palaeozoic cover in the Uralides and its western foredeep (Figs. 2, 3; Gafarov 1970; Glasmacher et al. 1999, 2001a; Nikishin et al. 1996, 1997; Puchkov 1997; Roberts and Siedlecka 2002). The Riphean and Lower Vendian are characterized by the development of deep, wide troughs within a thick continental crust due to epicontinental rifting (Maslov et al. 1997). Extension was accompanied by the formation of sub alkaline basalts or a rhyolite-basalt series of continental affinities (Goldin et al. 1973; Garris 1977; Parnachev 1981; Parnachev et al. 1981; Alekseyev 1984; Alekseyev and Alekseyeva 1988; Getsen et al. 1987; Ivanov 1987, Sobolev 1996). Sedimentary complexes are dominated by shallow-water quartzites, subarkoses,

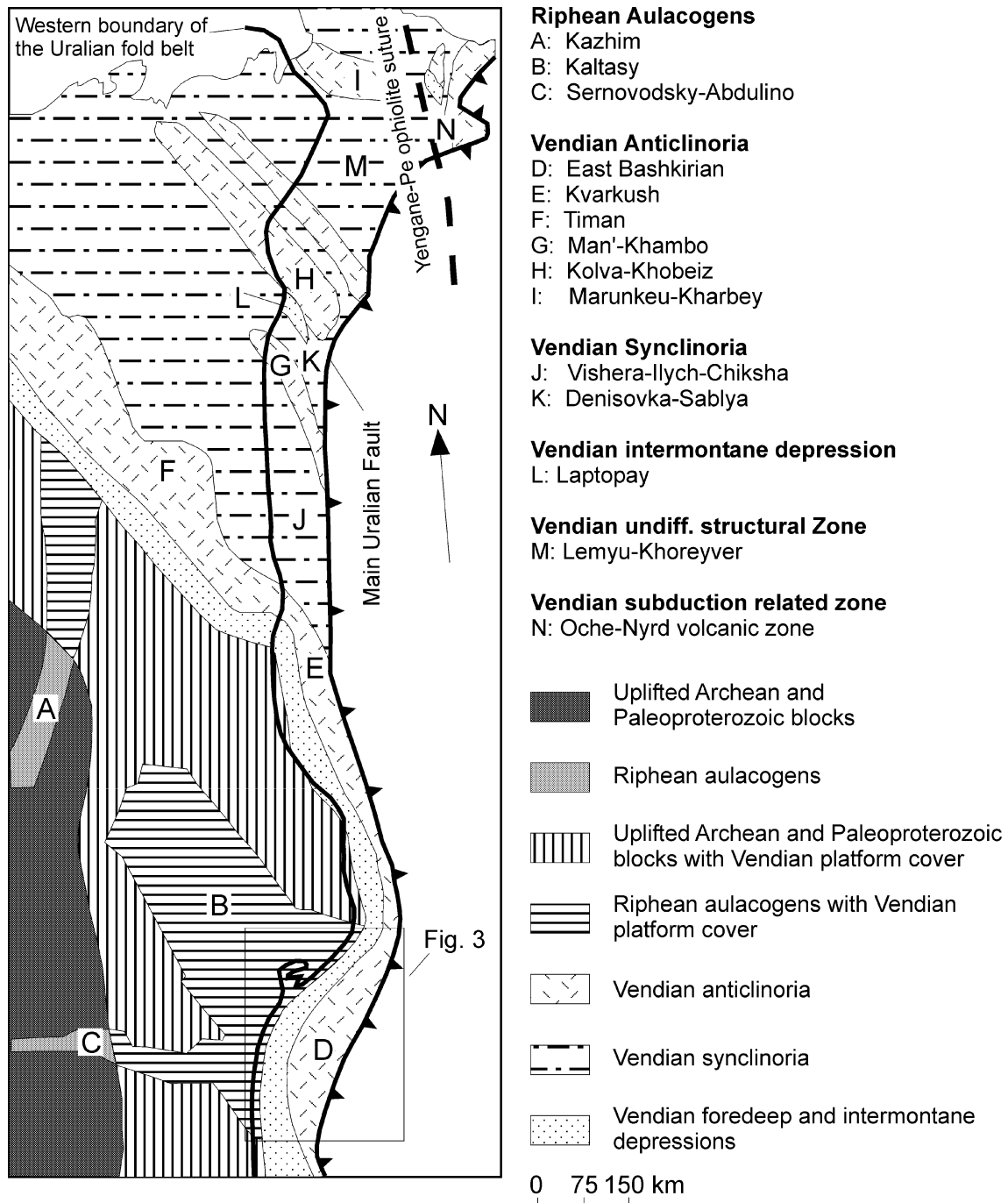
U. A. Glasmacher (✉)  
Forschungsstelle Archäometrie der Heidelberger Akademie  
der Wissenschaften am Max-Planck-Institut für Kernphysik,  
Postfach 103980, 69029 Heidelberg, Germany  
e-mail: ua.glasmacher@mpi-hd.mpg.de  
Tel.: +49-6221-516321  
Fax: +49-6221-516633

W. Bauer  
Geologisches Institut, RWTH Aachen,  
Wüllnerstrasse 2, 52056 Aachen, Germany

N. Clauer  
Centre de Géochimie de la Surface (CNRS-ULP),  
1 rue Blessig, 67084 Strasbourg, France

V. N. Puchkov  
Geological Institute of the Ufimian Geoscience Center,  
Russian Academy of Sciences,  
Karl Marx Str. 16/2, 450000 Ufa, Russia

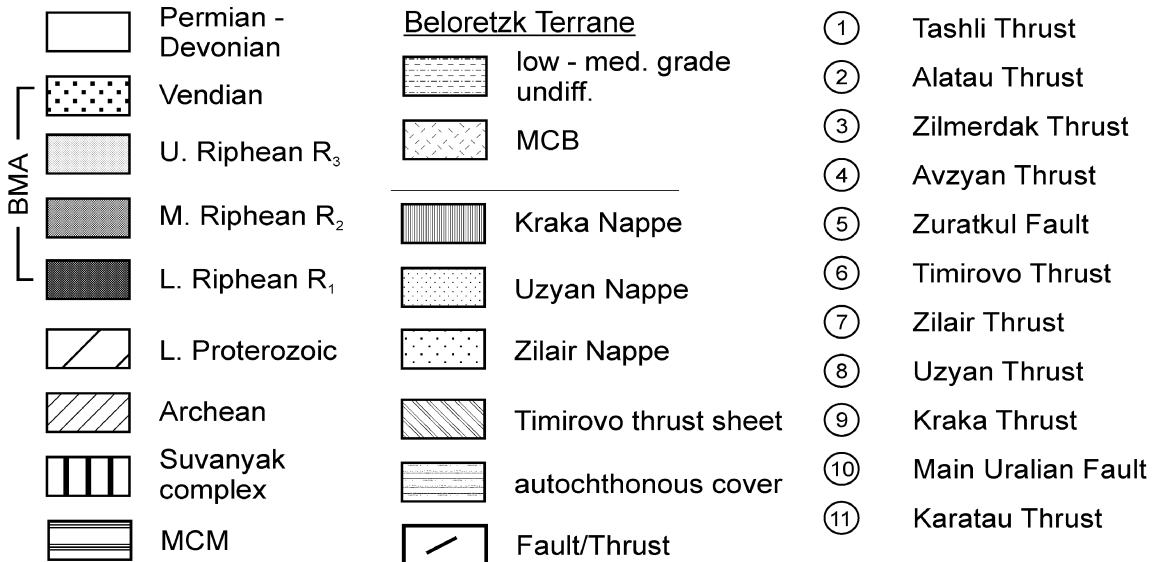
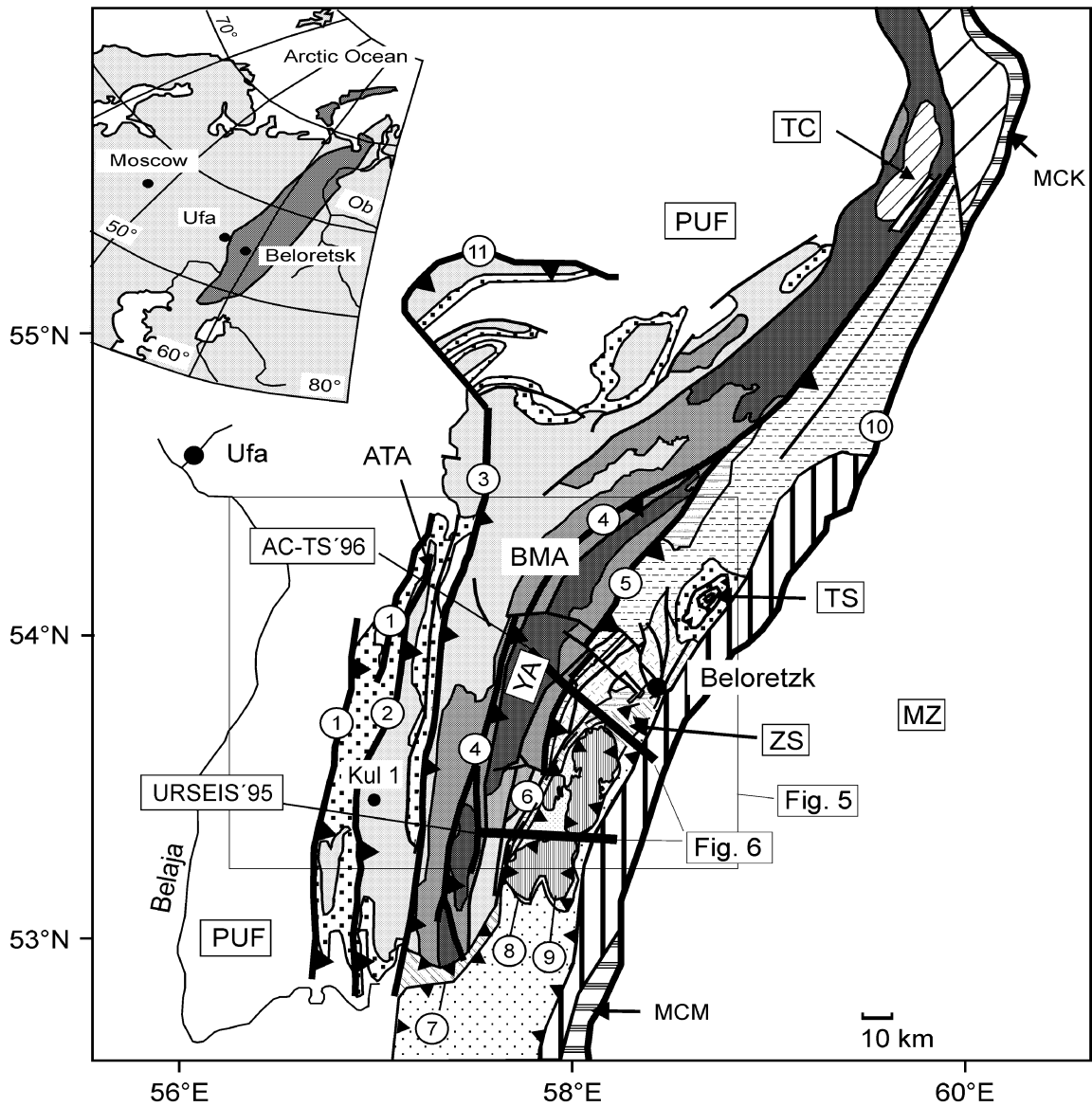




**Fig. 2** Schematic tectonic zonation of the pre-Late Proterozoic basement structures of the eastern part of the East European Craton (Puchkov 1997). Enclosed is the western limit of the Uralian orogen and the Main Uralian Fault

**Fig. 1** Tectonic overview map showing the major geological features of the East European Craton (EEC) and its relationship with the Phanerozoic orogens of Europe. *PM* Porkalla Mantsala Fault, *LR* Ladago Rift. Insert shows major terranes of the EEC (Gee and Zeyen 1996; Gorbatshev and Bogdanova 1993; Murell 2003)

arkoses, bioherm algal limestones, and dolomites. The Upper Vendian foredeep is filled with polymictic siliciclastic sediments and evaporites. The three graben-like structures: the Kazhim, Kaltasy and Sernovodsk-Abdulino aulacogens occur within the crystalline basement of the Volgo-Uralia Terrane. These aulacogens are up to 10 km deep and are partly overlain by up to 2 km of Vendian siliciclastic sediments (Romanov and Isherskaya 1994).



The partly deformed and metamorphosed Meso- and Neoproterozoic rocks in the western fold-and-thrust belt of the Uralides belong to the 'Douralides' tectonic complex of Kheraskov (1967). As a synonym, Puchkov (1997) used Pre-Uralides and 'Timanides'. Recently the term Timanian was also applied for Neoproterozoic (Late Vendian) deformation at the northeastern margin of the EEC in the Uralian Orogen (Roberts and Siedlecka 2002). In Upper Vendian time, a more than 2,000-km-long orogenic belt, which is called in the following as the Timanian Orogen, has formed at the eastern margin of the EEC. The main structural elements of the Timanian Orogen are: the East Bashkirian, Kvarkush, Timan, Man'-Khambo, Kolva-Khobeiz and the Marunkeu-Kharbey anticlinorium; the Vishera-Ilych-Chiksha and Denisovka-Sablya synclinorium; the Laptopy intermontane depression; the Lemyu-Khoreyver undifferentiated zone; the Yengane-Pe ophiolite suture and the Oche-Nyrd subduction-related volcanic zone (Fig. 2).

In the western fold-and-thrust belt of the southern Uralides, sedimentary, metamorphic and magmatic rocks of Riphean and Vendian age occur in the Bashkirian Mega-anticlinorium (BMA) and the Beloretzk Terrane (Fig. 3). Whereas, Glasmacher et al. (2001a) discussed in detail the polyphase Meso- and Neoproterozoic metamorphic and deformational evolution of the Beloretzk Terrane, the age of metamorphism (up to greenschist facies) and deformation in the eastern BMA has not been constrained by isotopic dating. Related to the spatial orientation of the structures, the cleavage formation and the incipient and greenschist-facies metamorphism were assigned to the Uralian deformation (Giese et al. 1999; Matenaar et al. 1999).

The isotopic dating of incipient metamorphism and the development of slaty cleavage in siliciclastic rocks using the K-Ar dating technique was demonstrated by many authors (Clauer 1974; Kralik 1983; Kligfield et al. 1986; Reuter 1987; Toulkeridis et al. 1994; Clauer et al. 1995; 1997; Zhao et al. 1997, 1999; Jaboyedoff and Cosca 1999; Glasmacher et al. 2001b and references herein). A long practice (since Clauer 1974, and discussions in Clauer and Chaudhuri 1995, 1998) of studying different types of siliciclastic rocks from diagenetic to low-grade metamorphic domains, has emphasized the need of combined studies including careful separation of potassic white mica and clay mineral size fractions with detailed XRD mineralogical and electron microscopical observations (SEM and TEM) to support the K-Ar isotopic determinations. Indeed, interpretation of K-Ar data of potassic white mica and clay mineral size fractions have to consider mixtures of detrital and authigenic mineral compo-

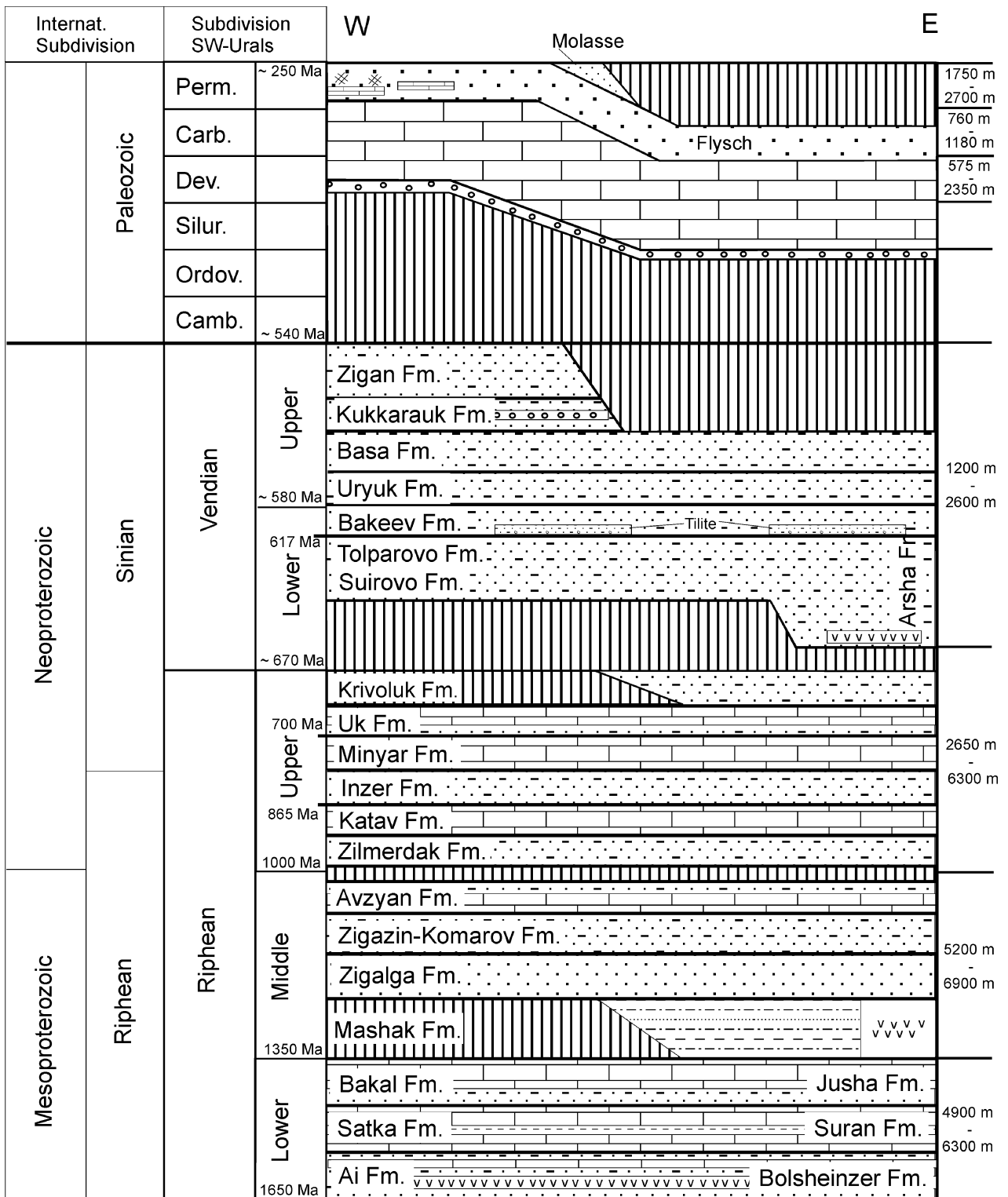
nents, as well as the thermal and deformational overprint of the siliciclastic rocks. As long as the thermal overprint has not reached the closure temperature of the clay minerals and potassic white mica and no deformation has happened, the isotopic system of these grains carry either preferentially detrital-age information or mixed information integrating detrital and authigenic ages. If deformation causes recrystallization of the clay minerals and potassic white mica below the closure temperature, the degree of resetting the isotopic system in a given volume depends on the ratio between the total volume of the cleavage domains and the total volume of the microlithon zones (Huon et al. 1987, 1993; Schaltegger et al. 1994, Clauer et al. 1995). Leitch and McDougall (1979) found that metapelites, which had experienced temperatures of about 300 °C, were completely reset. In addition, Hunziker et al. (1986) reported a complete Ar release temperature of 260 (30) °C for <2 µm particles of detrital illite in slates.

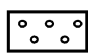
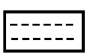

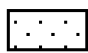
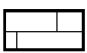

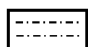
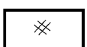
This paper presents K-Ar determinations on illite and fine-grained potassic white mica of Meso- and Neoproterozoic siliciclastic rocks from the western fold-and-thrust belt of the southern Urals to provide information about the evolution of various metasedimentary rock types constitutive of the eastern BMA and the Beloretzk Terrane. Petrography, rock foliation, as well as Kübler index and Árkai index analyses were conducted to provide supporting information necessary to interpret the K-Ar dates.

## Regional geology

The BMA, a broad NNE and SSW plunging antiformal structure, consists of more than 10,000-m-thick Meso- to Neoproterozoic siliciclastic and carbonate units that are formed in terrestrial fluvial to shallow marine environments (Figs. 3, 4 and 5; Kozlov 1982; Kozlov et al. 1989, 1995; Maslov et al. 1997). The thickness of the Zilmerdak Formation (lowermost Upper Riphean) varies strongly between about 600 m and over 3,000 m, west and east of the Zilmerdak thrust, respectively. Upper Vendian polymict siliciclastic units are interpreted as flysch and molasse deposits of a Neoproterozoic orogen at the eastern margin of EEC (Puchkov 1997; Stroink et al. 1997; Giese et al. 1999; Glasmacher et al. 1999, 2001a; Willner et al. 2001, 2003). The detritus of Riphean and Vendian sandstone from the BMA reflects the change of tectonic conditions in the Upper Vendian from a passive (since about 1,350 Ma) to a convergent continental margin within a presumed transpressional setting (Willner et al. 2001). The U-Pb age signature of detrital Riphean polycyclic rounded zircons is compatible with crystallization in the interval of 1.8–2.3 Ga, which is the significant age signature of the basement of the EEC. The majority of the polycyclic rounded zircons of Vendian sandstones have a similar Palaeoproterozoic U-Pb crystallization age as the Riphean. The U-Pb age signature and the internal magmatic growth zoning of euhedral zircons reflect a mag-

**Fig. 3** Geological map of the western part of the southern Urals (*ATA* Ala-Tau-Anticline, *BMA* Bashkirian Mega-anticline, *KC* Kraka Complex, *MCB* Metamorphic complex of Beloretzk, *MCK* Metamorphic complex of Kurtinsky, *MCM* Metamorphic complex of Maksyutov, *PUF* Pre-Uralian Foredeep, *TC* Taratash Complex, *TS* Tirlyan Synclinorium, *YA* Yamantau Anticlinorium, *ZS* Zilair Synclinorium, *MZ* Magnitogorsk Zone)



- |                                                                                     |              |                                                                                     |                        |                                                                                       |               |
|-------------------------------------------------------------------------------------|--------------|-------------------------------------------------------------------------------------|------------------------|---------------------------------------------------------------------------------------|---------------|
|  | Conglomerate |  | Shale/Slate            |  | Volcanic rock |
|  | Sandstone    |  | Limestone/<br>Dolomite |  | Hiatus        |
|  | Siltstone    |  | Salt                   |                                                                                       |               |

matic source between 643 and 512 Ma (Willner et al. 2003).

The Lower and Middle Riphean strata is cut by thick alkaline to subalkaline basic dikes of Late Middle Riphean age (about 1,050 Ma: K-Ar uralite, fine-grained amphibole age; Sobolev 1996). Additional dikes of Lower, Middle and Upper Riphean age (K-Ar whole rock or uralite ages) are described by Alekseyev (1984). Effusive magmatism is recorded for the lower part of the Lower Riphean (trachybasalts, trachybasalt porphyrite), the lower part of the Middle Riphean (~1,350 Ma, liparite-basalt suite) and Early Vendian (subalkaline basalts; Fig. 4).

In the west, the Tashli thrust separates the gently deformed Devonian to Permian strata (3,000 m thickness) of the Pre-Uralian Foredeep (PUF) from the intensely folded and partly metamorphosed Meso- to Neoproterozoic sedimentary rocks of the BMA (Fig. 5). In the east, the Zuratkul Fault separates the BMA from the Mesoproterozoic low- to high-grade metamorphic units of the allochthonous Beloretzk Terrane (Glasmacher et al. 1999, 2001a).

The BMA is characterized by the longitudinal N-S oriented Ala-Tau anticlinorium, Inzer synclinorium, and Yamantau anticlinorium (from west to east) that are separated by the Ala-Tau, Zilmerdak, and Avzyan thrusts. In the north, west and south of the Ala-Tau anticlinorium, Vendian flysch deposits are overlain by Devonian to Carboniferous siliciclastic and carbonate units of about 2,500 m thickness (Puchkov 2000). The Yamantau anticlinorium extends to the Kurgass anticline in the south, where an angular unconformity between the Riphean and Ordovician is recorded. Diagenetic to anchizonal grade was reached in the Ala-Tau anticlinorium, and the Inzer synclinorium, as well as lower greenschist metamorphic grade in the Lower and Middle Riphean sedimentary rocks of the Yamantau anticlinorium (Glasmacher et al. 1997, 2004; Matenaar et al. 1999; Glasmacher et al. 2004).

The Beloretzk Terrane, which is located east of the Zuratkul Fault, consists of a western low- to medium grade metamorphic part and an eastern medium- to high-grade metamorphic complex of Beloretzk (MCB). A Pb/Pb zircon age signature of a Riphean quartzite from the MCB indicate an Archaean zircon formation (3,070–2,480 Ma) which is interpreted as a further indication of the exotic nature with respect to the EEC of the MCB (Glasmacher et al. 2001a).

To the east and south of the BMA, the Zilair synclinorium forms a SW-plunging, broad synform of Ordovi-

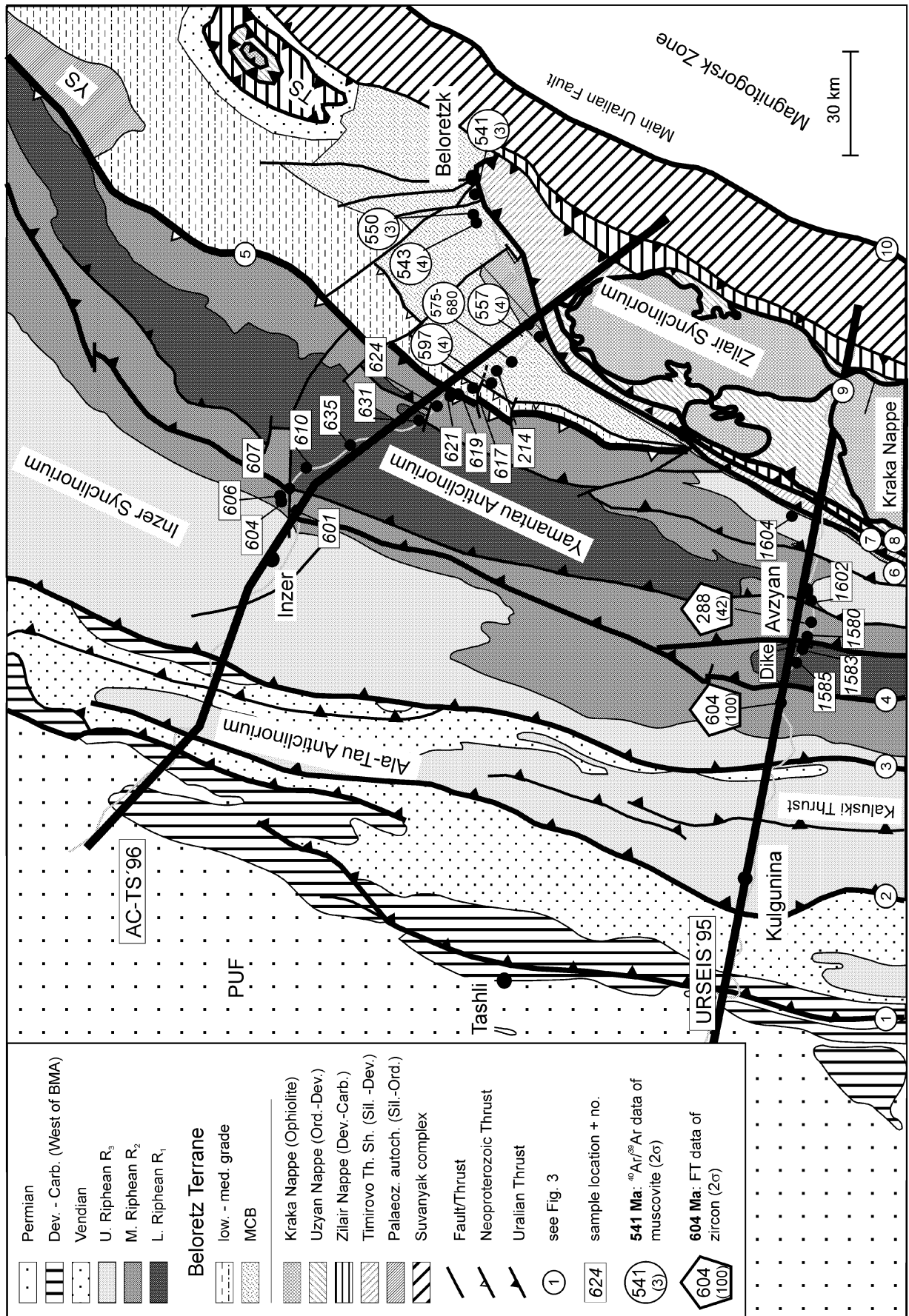
cian to Devonian siliciclastic and carbonate sedimentary rocks that unconformably overlie the Beloretzk Terrane (Figs. 4, and 5, Giese et al. 1999; Glasmacher et al. 2001a). Close to the unconformity at the AC-TS'96 transect, the Ordovician and Silurian sedimentary rocks are almost undeformed. The deformation increases towards the east and along strike towards the south. The first major thrust is located at the base of the Devonian limestones. To the east of this thrust, all rocks show NW-vergent folding and axial-planar cleavage. The Late Devonian Zilair flysch that increases in thickness towards the south, forms the entire core of the synclinorium (Brown et al. 1996; Bastida et al. 1997; Puchkov 1997). Brown et al. (1998) distinguished a Zilair nappe and a basal Timirovo thrust system (Fig. 5). The Zilair nappe is overthrust by the Uzyan nappe, an imbricated unit of Ordovician to Devonian continental rise sedimentary rocks. Separated by a basal melange, the Kraka ophiolite complex, a nappe of unknown age, overlies the Uzyan nappe. The post-Uralian exhumation history was described by Glasmacher et al. (2002).

## Sample description and analytical methods

To cover the various metamorphic grades and the various degrees of cleavage fabric in the Yamantau anticlinorium central part of the BMA, eight slates, and nine phyllites were selected out of 36 samples of the Yamantau anticlinorium and the Beloretzk Terrane along the AC-TS'96 and the URSEIS'95 transects (see Figs. 5, 6, and Table 1). The sample preparation implemented the recommendations of the Working Group on Illite Crystallinity (Kisch 1991). The use of the term Kübler index (KI;  $CIS-FWHM_{ill001ad}$ ) for illite crystallinity and Árkai index (AI;  $CIS-FWHM_{Chl002ad}$ ) for chlorite crystallinity is in accordance to the recommendations of the AIPEA nomenclature committee (Guggenheim et al. 2002). The 17 samples were cleaned, broken by hammer and grained with a rotary disk mill for 5 s. Short milling duration was applied to avoid, as much as possible, fragmentation of the coarser grains. The milled material was sieved at 63  $\mu\text{m}$  and the oversized grains were milled again. This grinding procedure was repeated until 100–200 g of size fraction <63  $\mu\text{m}$  were obtained. Separation of the <2- $\mu\text{m}$ -size fraction was made in Atterberg settling cylinders. The subfractions <0.2 and 0.8  $\mu\text{m}$  of the <2  $\mu\text{m}$  fractions were separated by continuous-flow super centrifugation. No cation saturation was applied to the separated fractions.

The bulk mineralogical composition of the <63 and <2- $\mu\text{m}$ -size fractions and the KI and AI of the <2- $\mu\text{m}$ -size fractions were determined by using a Siemens D 500 X-ray diffractometer at 35 kV and 30 mA  $\text{CuK}\alpha$  radiation. Single silicon crystals were used as mounts to minimize the background signal and allow the use of the recommended material thickness of 0.3  $\text{mg}/\text{cm}^2$  (Krumm and Buggisch 1991). Sedimented glass mounts were made with 1 ml of a homogenised size fraction-distillate water

**Fig. 4** Stratigraphic subdivision of the Meso- and Neoproterozoic and Palaeozoic in the western fold-and-thrust belt, SW Urals (according to Garris 1977; Krasnobayev 1986; Gorozhanin 1990,1995; Semikhatov et al. 1991; Gorokhov et al. 1995; Kozlov et al. 1989, 1995; Ovchinnikova et al. 1995, 1998; Maslov et al. 1997, 2001; Ovchinnikova and Gorokhov 2000; Zaitseva et al. 2000; international time-scale after Haq and Eysinga 1998); vertical hatching hiatus,  $\nu$  volcanic rocks



**Fig. 5** Geological map of the investigated area (based on 1:200,000 scale map, Giese et al. 1999). <sup>40</sup>Ar/<sup>39</sup>Ar-ages: Glasmacher et al. 1999, 2001a; FT-zircon ages: Seward et al. 1997





**Table 1** Description of Precambrian samples used for K-Ar dating. *R<sub>1js<sub>2</sub></sub>* Lower Riphean Jusha 2; *R<sub>1sr<sub>2</sub></sub>* Lower Riphean Suran 2; *R<sub>1sr<sub>3</sub></sub>* Lower Riphean Suran 3; *R<sub>1sr<sub>4</sub></sub>* Lower Riphean Suran 4; *R<sub>1sr<sub>5</sub></sub>* Lower Riphean Suran 5; *R<sub>2mh</sub>* Middle Riphean Mashak; *R<sub>2av<sub>1</sub></sub>* Middle Riphean Lower Avzyan 1; *R<sub>2av<sub>2</sub></sub>* Middle Riphean Lower

Avzyan 2; *R<sub>2av<sub>4</sub></sub>* Middle Riphean Upper Avzyan 4; *R<sub>3in</sub>* Upper Riphean Inzer; *S<sub>1w</sub>* Silurian Wenlock; *ss* bedding, *S1* first cleavage, *S2* second cleavage, *L No.* locality number, *S No.* sample number (see Figs. 3, 4)

L No.	S No.	Longitude (east)	Latitude (north)	Stratigraphy	Lithology	ss (°)	S1 (°)	S2 (°)
AC-TS'96-transect (eastern part)								
Yamantau anticlinorium								
601	2224	~54°11'60"N	~57°39'00"E	R <sub>2av<sub>2</sub></sub>	Black slate	Yes	Yes	No
604	2221	54°12'30"N	57°40'88"E	R <sub>2av<sub>2</sub></sub>	Black slate	Yes	150/43	No
606	2165	~54°12'70"N	~57°42'30"E	R <sub>2av<sub>1</sub></sub>	Black slate	331/47	114/36	No
607	2166	~54°12'30"N	~57°43'60"E	R <sub>2av<sub>1</sub></sub>	Black slate	Yes	Yes	No
610	2217	~54°11'50"N	~57°45'40"E	R <sub>1sr<sub>2</sub></sub>	Black phyllite	Yes	096/56	Yes
635	2215	~54°10'00"N	~57°45'90"E	R <sub>1sr<sub>2</sub></sub>	Black phyllite	280/73	114/64	132/64
631	2210	~54°07'30"N	~57°47'00"E	R <sub>1sr<sub>3</sub></sub>	Black phyllite	Yes	135/44	Yes
624	2205	~54°04'90"N	~57°49'40"E	R <sub>1sr<sub>5</sub></sub>	Black phyllite	276/26	Yes	Yes
621	2200	53°59'47"N	57°51'67"E	R <sub>1sr<sub>4</sub></sub>	Black phyllite	320/72	Yes	Yes
Beloretzk Terrane								
619	2199	~53°57'90"N	~57°52'00"E	R <sub>1sr<sub>4</sub></sub>	Black phyllite	110/78	100/90	315/20; strong shear fabric, top to E
617	2197	53°57'33"N	57°52'25"E	R <sub>1sr<sub>4</sub></sub>	Black phyllite	314/88	314/70	Strong shear fabric, top to E
214	2060	53°56'57"N	57°54'31"E	R <sub>2mh</sub>	Black phyllite	304/71	S1=ss	Strong shear fabric, top to E
URSEIS'96-transect (western part)								
Yamantau anticlinorium								
1585	2350	53°32'7"N	57°20'7"E	R <sub>1js<sub>2</sub></sub>	Black slate	274/16	241/36	No
1583	2352	53°32'1"N	57°23'0"E	R <sub>1js<sub>2</sub></sub>	Black slate	047/45	076/66	Yes
1580	2353	53°31'0"N	57°25'9"E	R <sub>2av<sub>1</sub></sub>	Black phyllite	092/83	S1=ss	No
1602	2359	53°31'0"N	57°29'7"E	R <sub>2av<sub>4</sub></sub>	Black slate	310/60	S1=ss	No
1604	2361	53°31'0"N	57°40'7"E	R <sub>3in</sub>	Grey slate	228/22	287/85;	242/34
							strong	

suspension (147 mg/100 ml equals 0.3 mg/cm<sup>2</sup>), and air-dried at room temperature. Each mount was scanned from 3 to 63° 2 $\theta$  at a scan-rate of 0.6° 2 $\theta$ /min. After determination of the air-dried crystallinity, the samples were left at a temperature of 60 °C for 4 h in an ethylene glycol-saturated atmosphere, and the KI and AI were measured again.

The FWHM<sub>Ill001ad</sub>, FWHM<sub>Ill001gly</sub>, FWHM<sub>Chl002ad</sub> and FWHM<sub>Chl002gly</sub> were determined as the median value of nine measurements of the full width at half height maximum ( $^{\circ}\Delta 2\theta\text{CuK}\alpha$ ) of the 10 Å peak (Illite<sub>001</sub>) and 7 Å peak (Chlorite<sub>002</sub>). The peak heights were measured by using an ASSEMBLER-program, which was programmed for the DACO-MP (Frank 1987). Calibration of the analytical procedure was made using the recommended standard samples (Warr and Rice 1994). Shortly after measuring the samples, the standards were measured 45 times. All data were recalculated to CIS-data. The conversion equations are available from the first author. The boundary between diagenesis and anchizone was set at CIS-FWHM<sub>Ill001ad</sub>=0.42

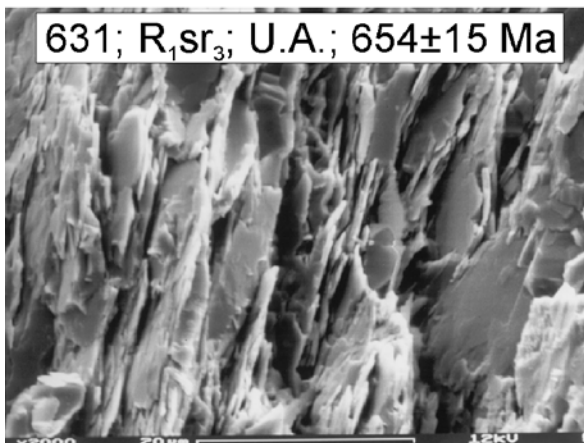
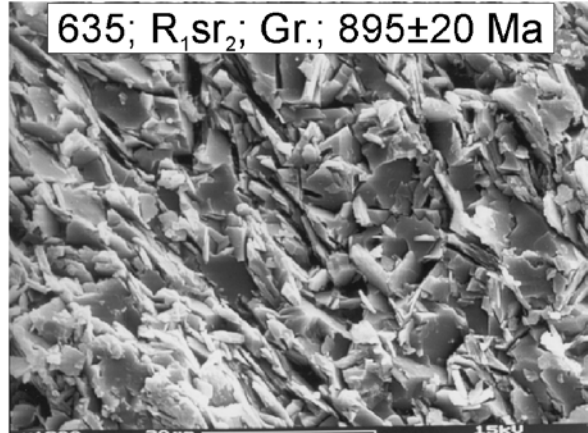
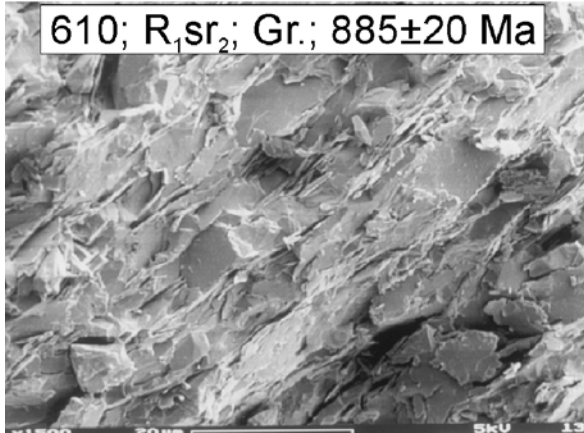
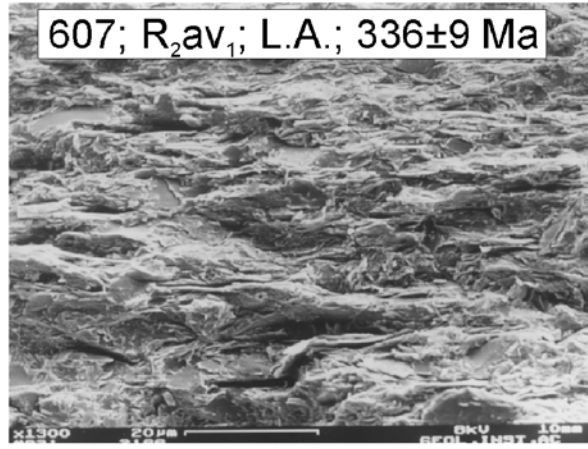
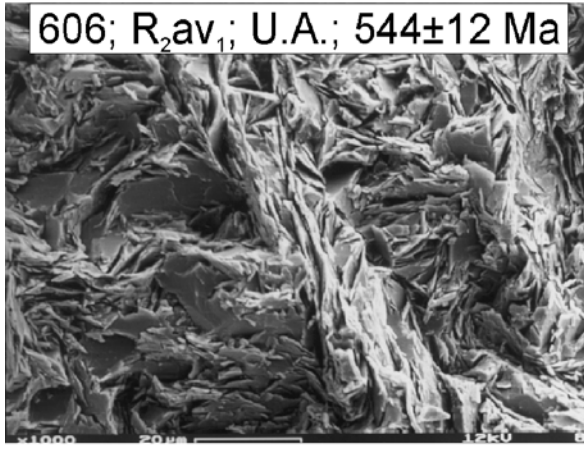
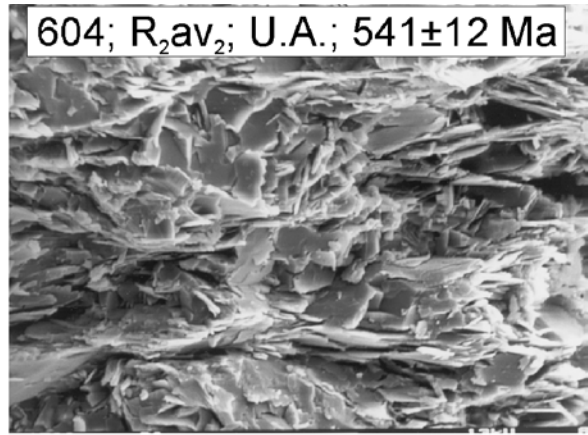
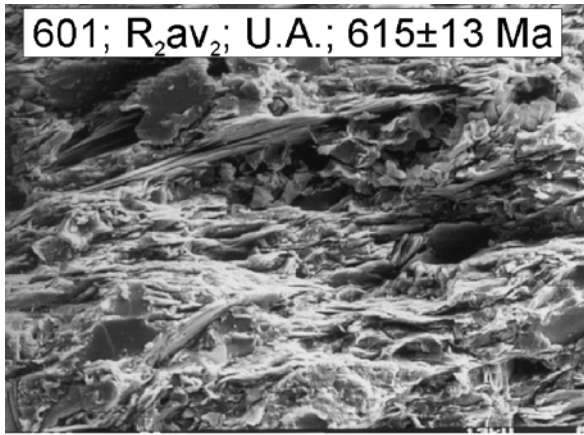
( $^{\circ}\Delta 2\theta\text{CuK}\alpha$ ), and that between anchizone and epizone at CIS-FWHM<sub>Ill001ad</sub> = 0.25 ( $^{\circ}\Delta 2\theta\text{CuK}\alpha$ ; Warr and Rice 1994). Boundary values of chlorite crystallinity—diagenesis/anchizone: CIS-FWHM<sub>Chl002ad</sub>=0.33 ( $^{\circ}\Delta 2\theta\text{CuK}\alpha$ ), CIS-FWHM<sub>Chl002ad</sub>=0.26 ( $^{\circ}\Delta 2\theta\text{CuK}\alpha$ )—were used as described by Árkai (1991) and Árkai et al. (1995, 1996).

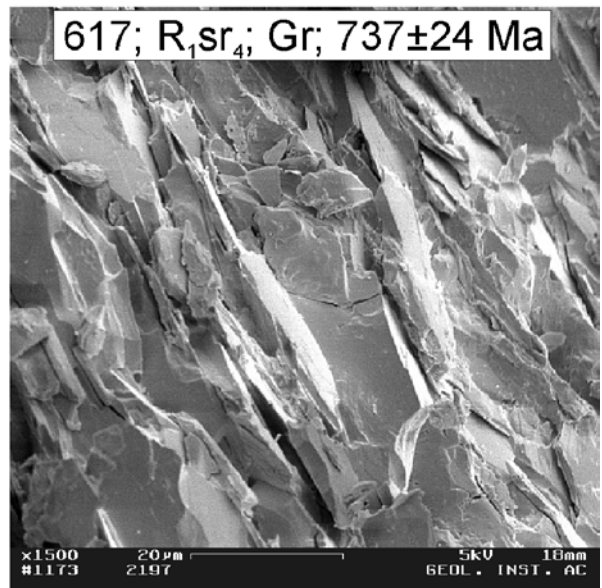
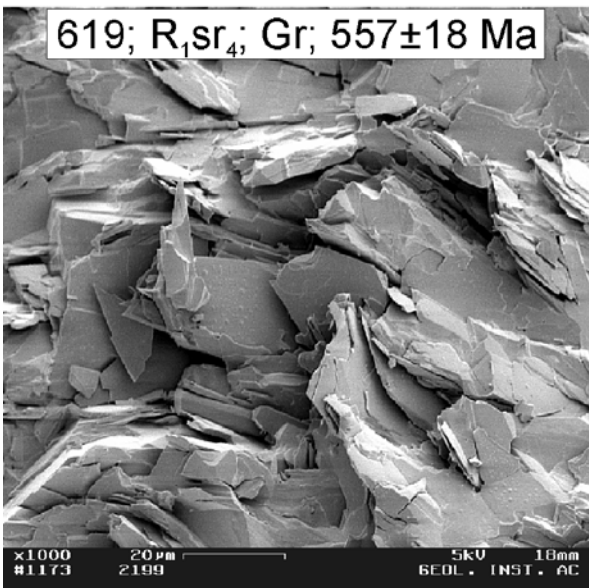
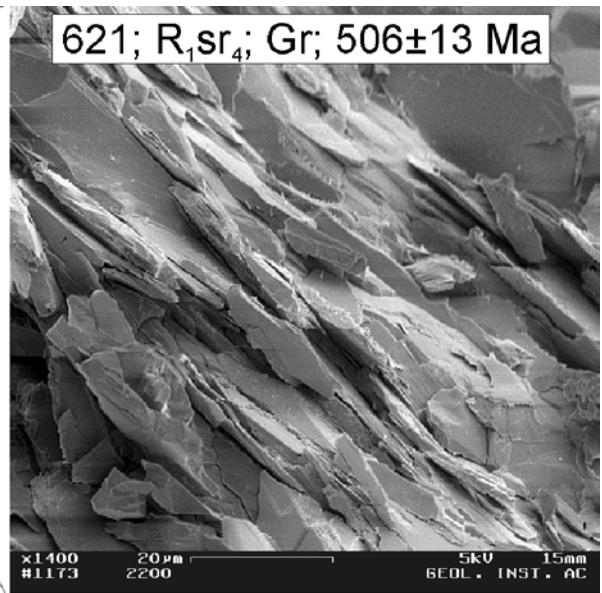
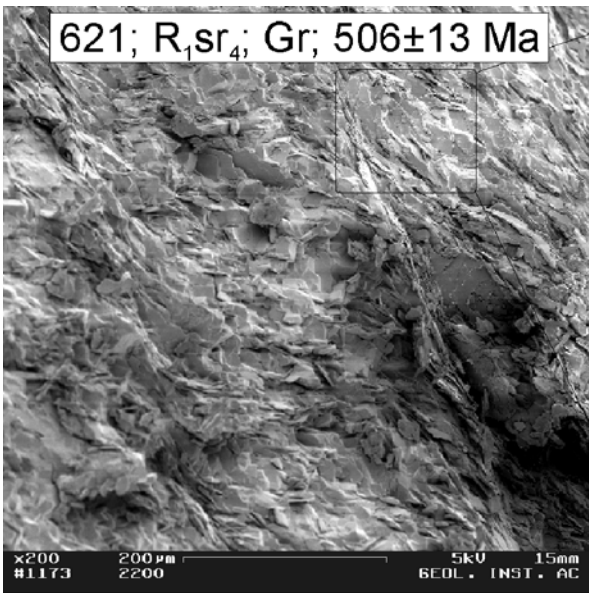
The rock foliation was observed at microscopic scale at a Zeiss DSM962 at the Geologisches Institut, RWTH Aachen, Germany. Rock specimens were broken either perpendicular to the sedimentary foliations or perpendicular to the cleavage planes. The broken surfaces were covered with gold. SEM-images were taken at various magnifications. The magnification 1,000–1,600 was chosen to display the foliations relevant for the interpretation of the K-Ar dates (Figs. 7, 8 and 9). The classification systems of Powell (1979), Borradaile et al. (1982), and Passchier and Trouw (1996) were applied to describe the foliations.

K-Ar isotopic analyses were made using a procedure close to that developed by Bonhomme et al. (1975). Potassium was measured by atomic absorption with a general accuracy of  $\pm 1.5\%$ . For Ar analysis, the samples were pre-heated under high vacuum at 100 °C for at least 12 h to reduce the amount of atmospheric Ar adsorbed on the

◀ **Fig. 6** Detailed geological maps of the area surrounding the sample location at the AC-TS'96 transect and the URSEIS'95 transect. Shown are also the sample locations, sample location numbers, stratigraphic age, K-Ar ages and metamorphic grade determined by clay mineral crystallinity, vitrinite reflectance and conodont colour alteration index. Metamorphic data along the AC-TS'96 transect are described by Glasmacher et al. (1997) and Matenaar et al. (1999). *PUF* Pre-Uralian Foredeep, *ATA* Ala-Tau Anticlinorium, *IS* Inzer Synclinorium, *YA* Yamantau Anticlinorium, *Pa* Parautochthon, *ZS* Zilair Synclinorium, *TS* Tirlyan Synclinorium, *Kul 1* drill hole Kulgunina 1

**Fig. 7** SEM-images of slates and phyllites along the AC-TS'96 transect. The images display various degrees of cleavage development. See text for further explanation. (601/location number, R<sub>2av<sub>2</sub></sub> stratigraphic position, UA upper anchizone, Gr greenschist facies, K-Ar-age $\pm 2\sigma$ ) ▶





**Table 2** Mineral composition of size fractions <63  $\mu\text{m}$ . Symbols: XX major = >20%, X minor = <20%, ac accessory = <5%, - not detected, An Anorthite, w-M potassic white mica with the exception of illite)

L No.	S No.	Strat.	Qtz	K-Fsp	Alb	An	w-M	Ill	Chl	Cal	Dol	Hem
AC-TS'96-transect (eastern part)												
Yamantau anticlinorium												
601	2224	R <sub>2</sub> av <sub>2</sub>	xx	x	-	-	x	xx	xx	-	-	-
604	2221	R <sub>2</sub> av <sub>2</sub>	xx	-	x	-	x	xx	xx	-	-	-
606	2165	R <sub>2</sub> av <sub>1</sub>	xx	x	-	-	ac	xx	xx	-	-	-
607	2166	R <sub>2</sub> av <sub>1</sub>	xx	x	-	-	x	xx	-	-	-	x
610	2217	R <sub>1</sub> sr <sub>2</sub>	xx	-	x	-	xx	-	xx	x	x	-
635	2215	R <sub>1</sub> sr <sub>2</sub>	xx	x	x	-	xx	-	x	-	-	-
631	2210	R <sub>1</sub> sr <sub>3</sub>	xx	ac	x	-	xx	-	xx	-	-	ac
624	2205	R <sub>1</sub> sr <sub>5</sub>	xx	-	-	ac	xx	-	-	x	x	-
621	2200	R <sub>1</sub> sr <sub>4</sub>	xx	-	-	-	xx	-	xx	-	-	-
Beloretzk Terrane												
619	2199	R <sub>1</sub> sr <sub>4</sub>	xx	-	-	ac	xx	-	xx	-	-	-
617	2197	R <sub>1</sub> sr <sub>4</sub>	xx	-	xx	xx	xx	-	x	x	-	-
214	2060	R <sub>2</sub> mh	xx	-	-	-	xx	x	-	-	-	-
URSEIS'96-transect (western part)												
Yamantau anticlinorium												
1585	2350	R <sub>1</sub> js <sub>2</sub>	xx	ac	x	-	-	xx	x	-	-	-
1583	2352	R <sub>1</sub> js <sub>2</sub>	xx	ac	x	-	-	xx	ac	-	-	-
1580	2353	R <sub>2</sub> av <sub>1</sub>	xx	ac	-	-	xx	-	-	-	-	-
1602	2359	R <sub>2</sub> av <sub>4</sub>	xx	-	-	-	x	x	-	-	-	-
1604	2361	R <sub>3</sub> in	xx	-	-	-	-	xx	x	-	-	-

mineral surfaces during sample preparation and handling. Ar isotopic results were controlled by repetitive analysis of the international GL-O standard that averaged  $24.38 \pm 0.12 \times 10^{-6} \text{ cm}^3/\text{g STP}$  ( $2\sigma$ ) of radiogenic Ar for three determinations. The blank of the extraction lines and the mass spectrometers were also periodically determined, the amount of residual  $^{40}\text{Ar}$  being systematically below  $1 \times 10^{-7} \text{ cm}^3$ . The  $^{40}\text{Ar}/^{36}\text{Ar}$  ratio of the atmospheric Ar averaged  $300.7 \pm 1.5$  for three determinations. The usual decay constants were used for age calculations (Steiger and Jäger 1977) and the overall error of the K-Ar age determinations was evaluated to be better than 2%.

## Results

### Petrography and foliations

The stratigraphic ages of the fine-grained, grey and black slates and phyllites range from Lower (~1,450 Ma) to Upper Riphean (~830 Ma, Fig. 3). Sedimentary foliations are indicated by grain size variations and/or changes in mineral composition.

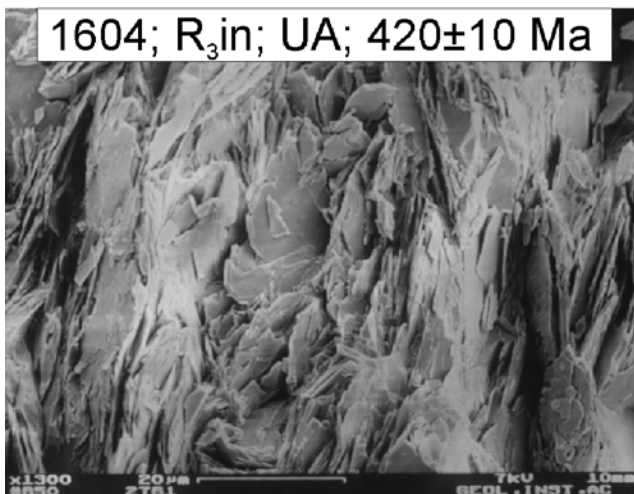
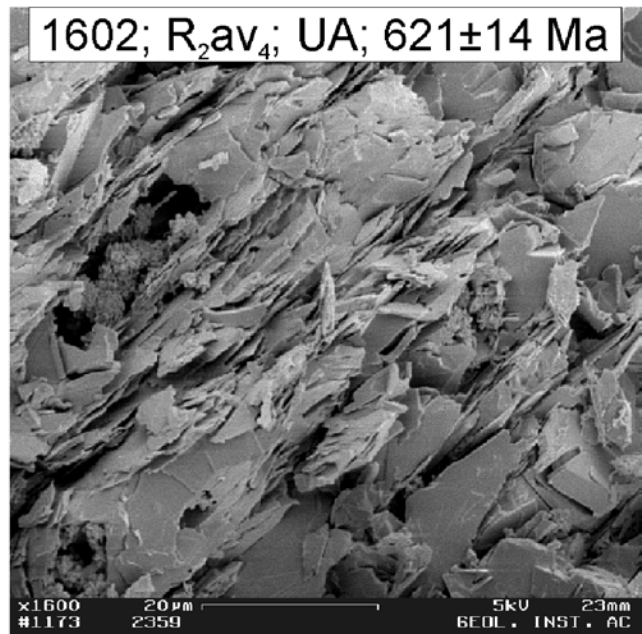
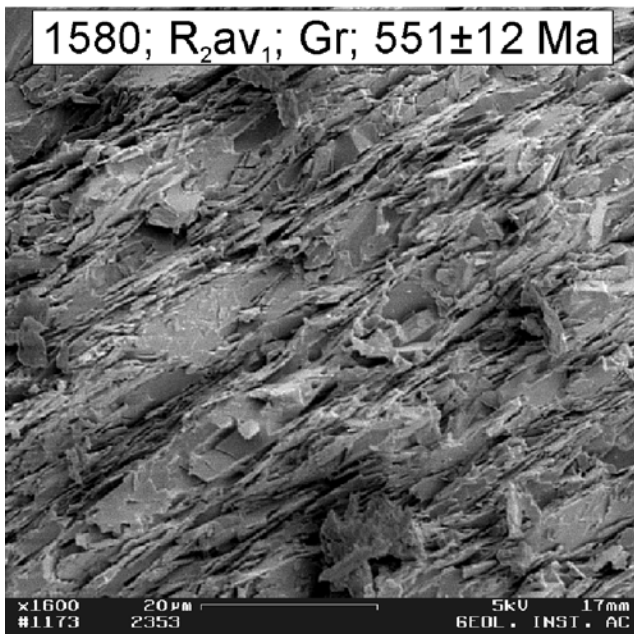
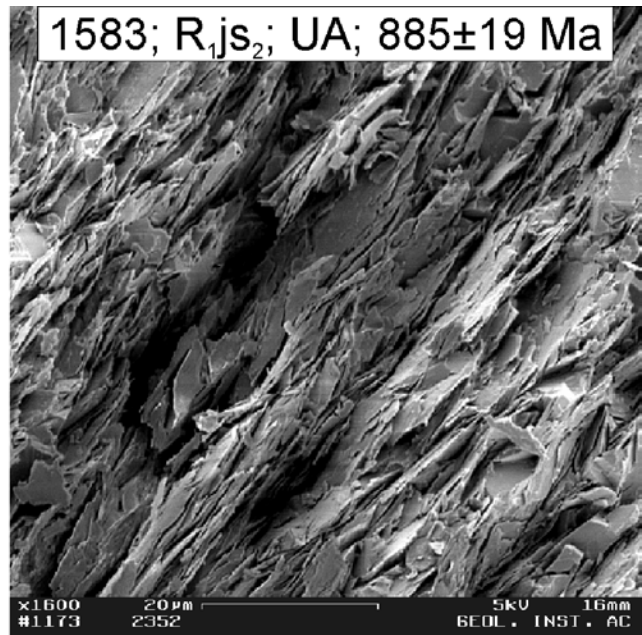
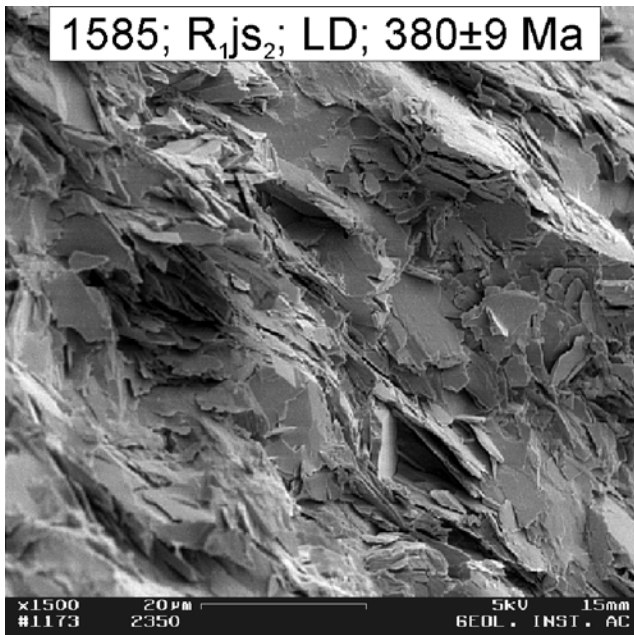
Lower Riphean phyllites (Table 2; Figs. 5, 6; locations #610, #635, #631, #624, #621, #619, #617) with quartz, potassic white mica and chlorite as the major and potassium feldspar, anorthite, albite and calcite, and dolomite as the minor to accessory mineral phases, were studied in the Yamantau anticlinorium and the Beloretzk Terrane along the AC-TS'96 transect. The mineral spectra of the Middle Riphean slates (locations #214, #601, #604, #606,

#607, #1602) along the AC-TS'96 and URSEIS'95 transects, are characterized by quartz, illite and chlorite as the major components and potassium feldspar, albite and fine-grained muscovite as the minor to accessory components. Fine-grained muscovite is the major mineral phase of the Middle Riphean phyllite (location #1580), in addition to quartz and chlorite. One Upper Riphean slate (location #1604) contains quartz, illite and minor amounts of chlorite.

Cleavage has overprinted the fine-grained bedding micro-foliation of the slates and phyllites (Table 1, Figs. 7, 8, 9). The Lower Riphean phyllites along the AC-TS'96 transect are characterized by coarse grain size (Figs. 7, 8 and Table 1). In addition, one Lower Riphean phyllite (location #635) shows well-crystallized grains. Two sets of cleavage planes are developed in all seven sample locations. The spacing of the first S1 cleavage planes varies between less than 5  $\mu\text{m}$  (locations #635, #631, #621) and more than 10  $\mu\text{m}$  (locations #610, #619, #617). The second cleavage S2, a shear cleavage, is wider in spacing (more than 300  $\mu\text{m}$ ) and has displaced the S1 planes (location #621; Fig. 7). A smaller grain size and a well-developed cleavage are typical for the Middle Riphean slates of the AC-TS'96 transect. In the Yamantau anticlinorium, one Middle Riphean slate (location 607) is characterized by a very fine-grain size and a very narrow spaced cleavage. In contrast, one Middle Riphean phyllite of the Beloretzk Terrane (location 214; Fig. 8) shows a coarser grain size and a well-developed narrow cleavage.

The Lower to Upper Riphean slates (locations #1585, #1583, #1602, #1604) and one phyllite (location #1580) of the URSEIS'95 transect are characterized by a well-developed cleavage (Fig. 9). The Lower Riphean slates (location #1585, #1583) are similar in the spacing of the cleavage planes and grain size. The spacing is narrower and the grain size smaller in the Middle Riphean Avzyan 1 slate (location #1580) than in the Middle Riphean

**Fig. 8** SEM-images of slates and phyllites along the AC-TS'96 transect. The images display various degrees of cleavage development. See text for further explanation. (635 location number, R<sub>1</sub>sr<sub>2</sub> stratigraphic position, UA upper anchizone, Gr greenschist facies, K-Ar-age  $\pm 2\sigma$ )



**Table 3** Mineral composition, Kübler and Árkai Index of the <2  $\mu\text{m}$  size fraction. CIS-FWHM<sub>Ill001ad</sub> = Kübler Index air dried, CIS-FWHM<sub>Ill001gly</sub> = Kübler Index glycolated, CIS-FWHM<sub>Chl002ad</sub> = Árkai Index air dried, CIS-FWHM<sub>Chl002gly</sub> = Árkai Index glycolated. SD standard deviation is related to repeated measurement

of the same sample. (*Meta grade* metamorphic grade, *LD* late diagenesis, *LA* lower anchizone, *UA* upper anchizone, *Green* greenschist facies, *w-M* potassic white mica with the exception of illite, *na* not analyzed)

L No.	S No.	Mineral composition of <2 $\mu\text{m}$ (sorted by relative abund., Qtz: accessory)	CIS-FWHM <sub>Ill001ad</sub> $^{\circ}\Delta 2\theta\text{CuK}\alpha$ (SD)	CIS-FWHM <sub>Ill001gly</sub> $^{\circ}\Delta 2\theta\text{CuK}\alpha$ (SD)	CIS-FWHM <sub>Chl002ad</sub> $^{\circ}\Delta 2\theta\text{CuK}\alpha$ (SD)	CIS-FWHM <sub>Chl002gly</sub> $^{\circ}\Delta 2\theta\text{CuK}\alpha$ (SD)	Meta grade
AC-TS'96-transect (eastern part)							
Yamantau anticlinorium							
601	2224	Ill, Chl, (Qtz)	0.321 (0)	0.321 (0)	0.308 (14)	0.306 (44)	UA
604	2221	Ill, Chl, (Qtz)	0.278 (16)	0.243 (16)	0.260 (11)	0.260 (11)	UA
606	2165	Ill, Chl, (Qtz)	0.312 (0)	0.312 (0)	0.292 (7)	0.308 (7)	UA
607	2166	Ill, (Qtz)	0.380 (31)	0.346 (21)	-	-	LA
610	2217	w-M, Chl, (Qtz)	0.243 (0)	0.209 (16)	0.244 (0)	0.244 (0)	Green
635	2215	w-M, Chl, (Qtz)	0.243 (0)	0.209 (14)	0.260 (7)	0.260 (7)	Green
631	2210	Ill, Chl, (Qtz)	0.278 (16)	0.243 (16)	0.276 (7)	0.260 (0)	UA
624	2205	w-M, (Qtz)	0.243 (0)	0.243 (0)	-	-	Green
621	2200	w-M, Chl, (Qtz)	0.243 (16)	0.243 (16)	0.260 (0)	0.244 (7)	Green
Beloretzk Terrane							
619	2199	w-M, Chl, (Qtz)	0.243 (16)	0.209 (16)	0.244 (7)	0.260 (0)	Green
617	2197	w-M, Chl, (Qtz)	0.243 (16)	0.209 (16)	0.252 (8)	0.244 (6)	Green
214	2060	w-M, Chl, (Qtz)	na	na	na	na	Green
URSEIS'96-transect (western part)							
Yamantau anticlinorium							
1585	2350	Ill, (Qtz)	0.450 (16)	0.450 (16)	-	-	LD
1583	2352	Ill, (Qtz)	0.279 (0)	0.279 (0)	-	-	UA
1580	2353	w-M, (Qtz)	0.244 (0)	0.244 (0)	-	-	Green
1602	2359	Ill, (Qtz)	0.278 (16)	0.244 (0)	-	-	UA
1604	2361	Ill, Chl, (Qtz)	0.279 (0)	0.279 (0)	0.277 (11)	0.285 (8)	UA

Avzyan 4 slate (location #1602). Two cleavage plane systems are developed in the Upper Riphean slate (location #1604). Both cleavage planes are tightly spaced and penetrative. The grain size of this slate is similar to that of the Middle Riphean Avzyan 4 slate.

#### Clay mineral composition, Kübler index and Árkai index

Fine-grained potassic white mica and chlorite are the main mineral phases of the <2- $\mu\text{m}$ -size fractions in all phyllites, and illite and chlorite in all slates (Table 3). Only quartz occurs as an accessory constituent. Feldspars were not detected by XRD analysis in any of the samples, which means that it is either not present or below the detection limit of about 3%.

Along the AC-TS'96 transect, the Kübler index (KI) of six Lower Riphean phyllites (locations #610, #635, #624, #621, #619, #617) of the Yamantau anticlinorium and Beloretzk Terrane indicates lower greenschist-facies metamorphic conditions—CIS-FWHM<sub>Ill001ad</sub>=0.243 (16)  $^{\circ}\Delta 2\theta\text{CuK}\alpha$ . One Lower Riphean phyllite is characterized by a KI of upper anchizone grade. After glycolation, the Kübler index value also indicates lower greenschist metamorphic conditions. The three Middle Riphean black

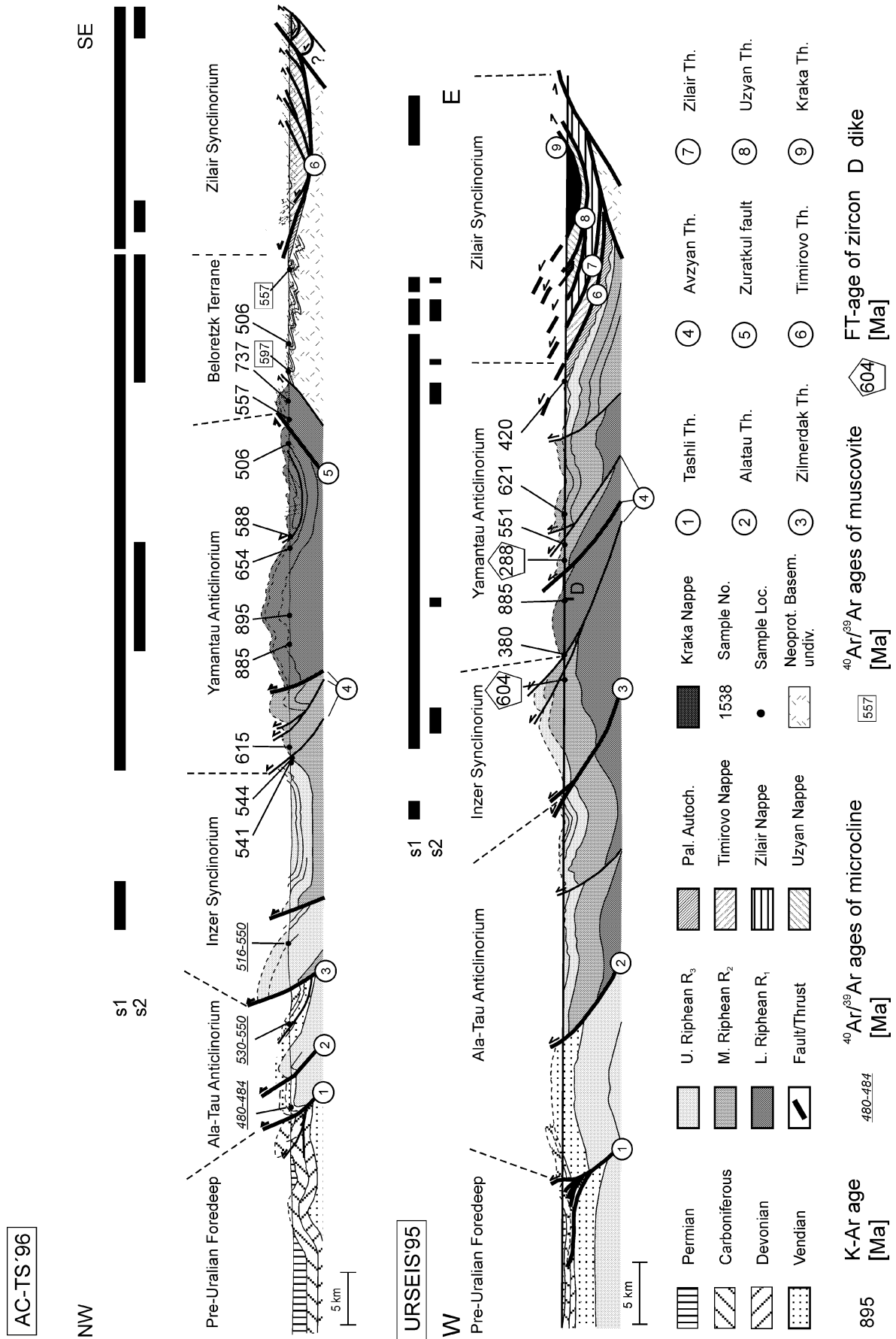
slates of the western part of the Yamantau anticlinorium (locations #601, #604, #606) are characterized by upper anchizone KI values—CIS-FWHM<sub>Ill001ad</sub>=0.278 (16)  $^{\circ}\Delta 2\theta\text{CuK}\alpha$  to 0.321 (0)  $^{\circ}\Delta 2\theta\text{CuK}\alpha$ —and one Middle Riphean black slate (location #607) by a lower anchizone KI value—CIS-FWHM<sub>Ill001ad</sub>=0.380 (31)  $^{\circ}\Delta 2\theta\text{CuK}\alpha$ .

Similarly, the metamorphic conditions of the black phyllite of the Beloretzk Terrane reached greenschist facies (Table 3). In addition, one (location #1580) of the Middle and Upper Riphean black slates reached the epizone—CIS-FWHM<sub>Ill001ad</sub>=0.244 (0)  $^{\circ}\Delta 2\theta\text{CuK}\alpha$ —along the URSEIS'95 transect. Three black slates (locations #1583, #1602, #1604) are characterized by upper anchizone KI values—CIS-FWHM<sub>Ill001ad</sub>=0.278 (16)  $^{\circ}\Delta 2\theta\text{CuK}\alpha$  to 0.279 (0)  $^{\circ}\Delta 2\theta\text{CuK}\alpha$ .

The Árkai index (AI) values are generally related to the measurements of the KI values for the high- and low-grade regions of the AC-TS'96 and URSEIS'95 transects. In areas of higher thermal grade, like the Yamantau anticlinorium, the AI yields values similar to the KI reflecting upper anchi- to epizone grades. As described by Árkai et al. (1995), “the ChC method is less sensitive for detecting differences in metamorphic grade than the IC method” of regions that underwent very low-grade metamorphism. Our experience dealing with samples of diagenetic and lower anchizone grade confirms this statement.

Local discordances of both parameters can be seen in the absolute values. The CIS-FWHM<sub>Chl002ad</sub> values of slates and phyllites frequently indicate either lower or higher metamorphic grade. As discussed by Merriman

**Fig. 9** SEM-images of slates and phyllites along the URSEIS'95 transect. The images display various degrees of cleavage development. See text for further explanation. (1585 location number,  $R_1$ / $js_2$  stratigraphic position, *LA* lower anchizone, *UA* upper anchizone, *Gr* greenschist facies,  $K$ -Ar-age $\pm 2\sigma$ )



**Fig. 10** Generalised WNW–ESE structural cross section along the AC-TS'96 and URSEIS'95 transect (location see Figs. 3, 5, Giese et al. 1999, <sup>40</sup>Ar/<sup>39</sup>Ar ages: Glasmacher et al. 1999, 2001a; FT-zircon ages: Seward et al. 1997)



**Table 4** Results of the K-Ar analyses [Ma ( $2\sigma$ )]. 20 mg of sample material was used to determine the potassium value and 25 mg of sample material was used to determine the Ar isotopic composition. For legend see Tables 3 and 1. Ar\* radiogenic Ar

L No.	S No.	Stratigraphic age (Ma)	Lithology	Meta grade	Size fraction ( $\mu\text{m}$ )	K <sub>2</sub> O (%)	Ar* (%)	<sup>40</sup> Ar* ( $10^{-6}$ cm <sup>3</sup> /g)	Age [Ma ( $2\sigma$ )]	
AC-TS'96-transect (eastern part)										
Yamantau anticlinorium										
601	2224	R <sub>2</sub> av <sub>2</sub>	~1050	Slate	UA	<2	8.14	98.68	192.04	615 (13)
604	2221	R <sub>2</sub> av <sub>2</sub>	~1050	Slate	UA	<2	6.75	96.80	137.34	541 (12)
604	2221	R <sub>2</sub> av <sub>2</sub>	~1050	Slate	UA	<0.8	7.16	97.52	155.00	571 (13)
606	2165	R <sub>2</sub> av <sub>1</sub>	~1050	Slate	UA	<2	7.62	98.23	155.86	544 (12)
606	2165	R <sub>2</sub> av <sub>1</sub>	~1050	Slate	UA	<0.2	6.95	96.06	134.54	518 (12)
607	2166	R <sub>2</sub> av <sub>1</sub>	~1050	Slate	LA	<2	3.27	89.88	38.89	336 (9)
610	2217	R <sub>1</sub> sr <sub>2</sub>	~1450	Phyllite	Gr	<2	5.45	98.44	200.72	885 (20)
635	2215	R <sub>1</sub> sr <sub>2</sub>	~1450	Phyllite	Gr	<2	5.81	97.77	216.91	895 (20)
635	2215	R <sub>1</sub> sr <sub>2</sub>	~1450	Phyllite	Gr	<0.8	5.35	97.24	208.13	924 (21)
631	2210	R <sub>1</sub> sr <sub>3</sub>	~1450	Phyllite	UA	<2	5.10	96.88	129.48	654 (15)
631	2210	R <sub>1</sub> sr <sub>3</sub>	~1450	Phyllite	UA	<0.8	4.55	97.17	132.01	730 (17)
624	2205	R <sub>1</sub> sr <sub>5</sub>	~1450	Phyllite	Green	<2	8.61	98.85	193.00	588 (13)
621	2200	R <sub>1</sub> sr <sub>4</sub>	~1450	Phyllite	Green	<2	3.55	92.21	66.60	506 (13)
Beloretzk Terrane										
619	2199	R <sub>1</sub> sr <sub>4</sub>	~1450	Phyllite	Green	<2	1.81	72.44	38.00	557 (18)
617	2197	R <sub>1</sub> sr <sub>4</sub>	~1450	Phyllite	Green	<2	4.44	66.85	130.28	737 (24)
214	2060	R <sub>2</sub> mh	~1350	Phyllite	Green	<2	2.83	8.04	53.30	506 (12)
URSEIS'96-transect (western part)										
Yamantau anticlinorium										
1585	2350	R <sub>1</sub> js <sub>2</sub>	~1500	Slate	LD	<2	5.60	96.44	76.25	380 (9)
1583	2352	R <sub>1</sub> js <sub>2</sub>	~1500	Slate	UA	<2	8.84	99.21	325.41	885 (19)
1580	2353	R <sub>2</sub> av <sub>1</sub>	~1050	Phyllite	Green	<2	7.76	97.92	161.13	551 (12)
1602	2359	R <sub>2</sub> av <sub>4</sub>	~1050	Slate	UA	<2	5.83	98.52	139.26	621 (14)
1604	2361	R <sub>3</sub> in	~830	Slate	UA	<2	8.44	97.77	128.58	420 (10)

and Peacor (1999), chlorite crystals, growing under high strain rate, are commonly characterized by subgrain boundaries and dislocations and, consequently, by a reduced crystallite thickness. In comparison to potassic white mica, significant differences in index values result in KI values better than AI values where low-grade metamorphism is associated with the development of tectonic fabrics. However, Wang et al. (1996) described enhanced AI relative to the KI in pelitic rocks by deformation. Nearly all slates and phyllites of the URSEIS'95 transect are characterized by an enhanced KI. The internal deformation indicated by the cleavage development led to a decrease in the AI.

#### K-Ar isotopic data

The K-Ar data determined for the <2, <0.8 and <0.2- $\mu\text{m}$ -size fractions (Figs. 5, 6, 10 and Table 4) range from 336 (9) to 924 (21) Ma along the AC-TS'96 and the URSEIS'95 transects. In general, the K-Ar dates decrease from the central part of the Yamantau anticlinorium (AC-TS'96) to both limbs (Fig. 10). Both limbs of the Yamantau anticlinorium are characterized by east (Avzyan thrust system) and west dipping thrusts (Zuratkul Fault system). The highest values (885–924 Ma) occur in Lower Riphean phyllites (locations #610, #635) and in a slate (location #1583) of the central Yamantau anticlinorium. The K-Ar dates of Lower and Middle Riphean phyllites (locations #631, #624, #621) and slates (locations #606, #604, #601) decrease to 506 and 518 Ma,

respectively, towards the eastern and western limbs. In the Beloretzk Terrane, the K-Ar data of black phyllites vary between 737 (24) and 506 (12) Ma. The highest K-Ar value was observed for a sample of the medium grade metamorphic part (location #617) and the lowest K-Ar value for the high-grade metamorphic part (location #621) just in the footwall of the Zuratkul Fault. One Middle Riphean slate (location #607) taken in the close vicinity of a major E–W trending fault, yields the lowest K-Ar value of 336 (9) Ma of the Yamantau anticlinorium.

Along the URSEIS'95 transect, a Lower Riphean slate (location #1583) sampled in the thermal aureole of a Precambrian mafic dike (Alekseyev 1984), yields the oldest K-Ar age of 885 (19) Ma. A Lower Riphean slate (location #1585) located close to the first Avzyan thrust, is characterized by a K-Ar age of 380 (9) Ma. The K-Ar values are at 551 (12) Ma (location #1580) and 621 (14) Ma (location #1602) in the central part of the Yamantau anticlinorium (URSEIS'95 transect). An Upper Riphean slate (location #1604), close to the Palaeozoic autochthonous cover sequence, is characterized by a K-Ar age of 420 (10) Ma.

The K-Ar results obtained here by analyzing the <2, <0.8 and 0.2  $\mu\text{m}$  fractions scatter despite the absence of detectable feldspar in the fractions. Therefore, the scatter may be attributed to dominant mica-type particles of detrital origin generated in a source area of Archaean and Precambrian age, which were more or less affected by later thermal (diagenesis to lower greenschist facies) and tectonic (Neoproterozoic and Uralian deformation) processes. The K-Ar isotopic system of these micas could

have been completely reset during such thermal and deformational overprints reaching upper anchizonal to greenschist intensity, or during the development of a continuous penetrative cleavage. The detrital micas could also have been mixed with clay-type minerals newly-formed during the mentioned late events. In the following chapter we will discuss the K-Ar data in the context of the thermal and deformational evolution of the samples.

## Discussion

The study of the Yamantau anticlinorium and the Beloretzk Terrane along two transects outlines a strong variation in metamorphic grade, intensity of cleavage and K-Ar ages of the Riphean siliciclastic units. Phyllites and slates from both transect reached upper anchizonal to greenschist-facies metamorphic conditions. At the AC-TS'96 transect, a Middle Riphean slate exceeded only slightly lower anchizonal conditions, and one Lower Riphean slate of the URSEIS'95 transect records only late diagenesis. Phyllites of the eastern limb of the Yamantau anticlinorium and of the Beloretzk Terrane yield two directions of spaced foliation (Fig. 10). The K-Ar data range from 924 (21) Ma to 336 (9) Ma. The Lower Riphean samples (#610, #635) of the AC-TS'96 transect that are characterized by a wider spacing of the S1 cleavage domains, coarser grain size and partly well-crystallized grains, provide the highest K-Ar values at 895 (20) Ma and 885 (20) Ma. Within the  $2\sigma$ -error, the age of 924 (21) Ma for the  $<0.8$  size fraction of the sample #635 is the same as the age of 895 (20) Ma for the  $<2$ - $\mu\text{m}$ -size fraction. Towards the limbs of the Yamantau anticlinorium at the AC-TS'96 transect, the Middle Riphean slates and Lower Riphean phyllites with smaller grain size and narrower S1 cleavage planes have K-Ar values between 506 (12) Ma and 654 (15) Ma. The change in grain size combined with the increased amount of cleavage domains relative to microlithons leads to a partial or complete resetting of pre-Late Neoproterozoic metamorphic K-Ar ages in the central Yamantau anticlinorium during the development of the strong S1 cleavage. The S1 cleavage at the eastern limb of the Yamantau anticlinorium formed during the Late Neoproterozoic orogeny (Giese et al. 1999; Glasmacher et al. 2001a). The second cleavage S2 is thought to be of Uralian origin. Bons (1988) noted that muscovite rarely shows evidence of intracrystalline slip and polygonization, and appears to be deformed by plastic and elastic processes causing rapid defect migration and crystal growth. This process would also allow the diffusion of Ar out of the system. Similarly, Merriman et al. (1995) found that potassic white mica rarely shows strain microtextures and appears to have a greater capacity than chlorite to store strain energy, enabling it to recover from subgrain development by grain boundary migration, i.e. dislocation creep. Furthermore, a relationship between metamorphic grade and strain was previously described by various authors (Nyk 1985; Roberts and Merriman 1985; Fernández-Caliani and Galán 1992).

At the western limb of the Yamantau anticlinorium, the origin of the S1 cleavage was discussed by Giese et al. (1999) as being developed during the Uralian deformation. Despite the differences in metamorphic grade (W-limb: upper anchizonal, E-limb: lower greenschist grade), the SEM images indicate a similar cleavage on both limbs. Even a penetrative cleavage with shear bands as indicated by the SEM images of one Middle Riphean slate (location #606, AC-TS'96) did not reset the K-Ar age beyond 518 (12) Ma at the western limb. The K-Ar data of the two size fractions ( $<2$ ,  $0.2 \mu\text{m}$ ) of location #606 decrease from 544 (12)–518 (12) Ma, respectively. Only one Middle Riphean slate of lower anchizonal grade taken in the close vicinity of an E–W trending fault is characterized by a very fine-grained diagenetic foliation, a penetrative cleavage and a K-Ar age of 336 (9) Ma. Therefore, it cannot be excluded that the S1 cleavage in Middle Riphean slates at the western limb of the Yamantau anticlinorium (AC-TS'96 transect), is of Late Neoproterozoic origin. The Uralian tectono-thermal resetting of Proterozoic K-Ar ages might have influenced only pelitic rocks in the vicinity of thrusts or faults.

Similarly, one Lower Riphean black slate of the URSEIS'95 transect, with a penetrative cleavage from an outcrop in the hanging wall of the westernmost thrust of the Avzyan thrust system has a K-Ar age of 380 (9) Ma. Árkai et al. (1997) described a decrease in illite crystallite size in the hanging wall of the Glarus thrust plane, Swiss Helvetic Alps. They suggested that strain-induced reduction in illite crystallite size resulted from intracrystal slip and subgrain formation. Alternatively, Árkai et al. (2002) suggested that the increase in metamorphic grade in the vicinity of nappe boundaries in the Central Alps was caused by high shear strain. Both processes would lead to Ar loss and therefore to a reset of the K-Ar data.

Fission-track data of zircon from a Middle Riphean sandstone close to the first Avzyan thrust in the eastern Inzer Synclinorium indicate an age of 604 (100) Ma (Figs. 5, 10; Seward et al. 1997). Kübler index values of surrounding Middle Riphean slates indicate a middle anchizonal grade (Glasmacher et al. 2004). Annealing of fission-tracks in zircon is a function of temperature, time and  $\alpha$ -radiation damage (Kasuya and Naeser 1988). The amount of  $\alpha$ -radiation damage increases with time and with uranium and thorium concentrations in zircon. Tagami and Shimada (1996) discussed a zircon partial annealing zone (ZPAZ) between  $\sim 230$  and  $320$  °C for a heating duration of about  $10^6$  years. Fission-tracks in zircon grains from Miocene to Pleistocene sandstones and Miocene to Pliocene rhyolites of two drill holes in a sedimentary basin in Japan give indications for a temperature above  $200$  °C for the lower limit of the ZPAZ at a stable temperature of about 1 Ma (Hasebe et al. 2003). Furthermore, results of laboratory annealing experiments point towards a similar temperature range of the ZPAZ (Yamada et al. 1995; Tagami et al. 1998). This temperature range of the ZPAZ well covers the anchi- to epi-zone. Fission-tracks in zircon grains with high  $\alpha$ -radiation damage start to anneal at temperatures between 150 and

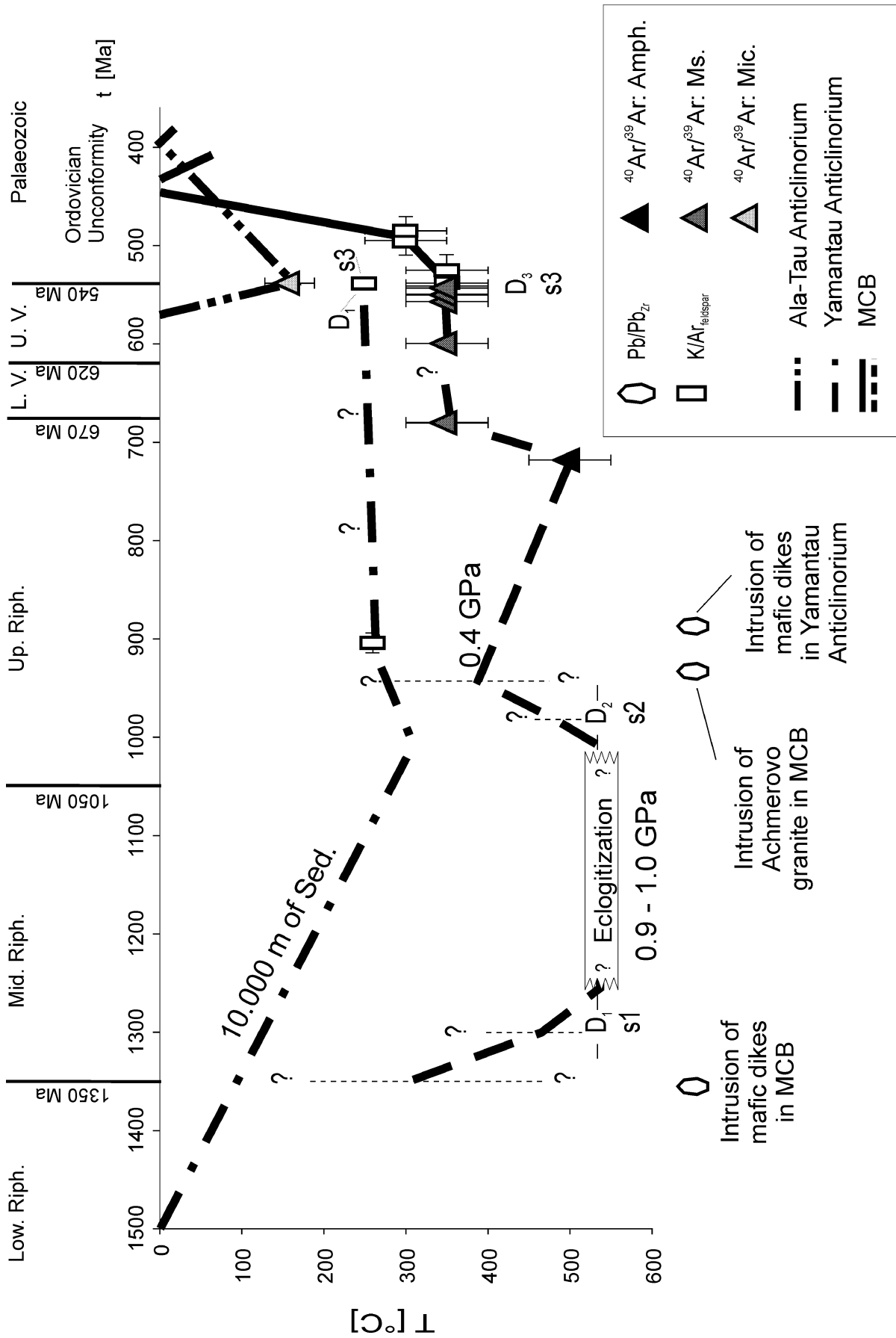
200 °C (Garver and Bartholomew 2001; Riley 2002). Therefore, a temperature of the middle anchizone at geological time scale ( $\sim 10^6$ – $10^7$  years) can partially anneal fission tracks in zircon. Complete annealing of fission tracks in zircon would need temperatures above 320 °C for duration of the thermal event in the range of 1–10 Ma (Tagami and Shimada 1996; Tagami et al. 1998; Rahn 2001; Brix et al. 2002).

Depending on the original detrital age, which must be older than 1,000 Ma, the anchizone condition in the Inzer synclinorium could have been reached in Neoproterozoic times. Between the first and second thrust of the Avzyan thrust system, a Lower Riphean slate (location #1583) of upper anchizone metamorphic grade with a well-defined cleavage is characterized by a K-Ar age of 885 (19) Ma (Fig. 10). This slate is located in the thermal aureole of a thick diabase dike of Precambrian age (Alekseyev 1984). In comparison, the metamorphic grade of the surrounding Lower Riphean slates is late diagenetic (Glasmacher et al. 2004). The age of the S1 cleavage is not known, but the strike and dip is similar to all S1 cleavage planes in the Yamantau anticlinorium that are of Late Neoproterozoic origin. However, the K-Ar values might result from a mixture of illite that grew or was reset during the intrusion of the diabase dike and partly reset during the development of the slaty cleavage. The age of the dike must be older than 885 (19) Ma. East of the main Avzyan thrust (second thrust), a Middle Riphean phyllite (locations #1580) provided a K-Ar age of 551 (12) Ma and a Middle Riphean slate (location #1602) of upper anchizone/epizonal metamorphic grade a K-Ar age of 621 (14) Ma (Fig. 9). Both pelitic rocks are pervasively sheared. The cleavage planes in the phyllite are narrowly spaced and the grain size is smaller than in the slate. Considering the grain size, and cleavage domains to microlithons ratio, the K-Ar data represent a partial reset of pre-Late Neoproterozoic metamorphic age—older than 621 (14) Ma—by a Late Neoproterozoic or younger deformation. In the hanging wall of the main Avzyan thrust, close to location # 1580, a zircon fission-track age of 288 (42) Ma from a Middle Riphean sandstone indicates movement along the Avzyan thrust in Early Permian time (Seward et al. 1997; Fig. 10). Prior to the Early Permian, the Middle Riphean units must have undergone a temperature of more than 320 °C, which agrees with the lower greenschist-facies metamorphic grade of the Middle Riphean black slates. The K-Ar age of 551 (12) of the <2- $\mu$ m-size fraction of the Middle Riphean phyllite (locations #1580) indicate that the lower greenschist metamorphic grade was reached in Precambrian times, whereas the zircon fission-track age of 288 (42) Ma indicates the final exhumation below about 200 °C in Permian times. If the intense internal deformation was caused by the Uralian orogeny, the K-Ar data should be reset to Devonian or Carboniferous values. As this is not the case, deformation should result from Late Neoproterozoic imprints.

Close to the overlying Palaeozoic autochthonous units, an upper anchizone Upper Riphean black slate, characterized by two sets of cleavage planes, yields a K-Ar age

of 420 (10) Ma. The second, wider spaced cleavage has the same direction as the first one in the Silurian slate of the Palaeozoic autochthonous units. Therefore, the K-Ar ages are interpreted as being caused by a mixture of pre-Late Neoproterozoic metamorphic fine-grained muscovite and illite grains that were partly reset by a Late Neoproterozoic and a Uralian internal deformation.

Lower Riphean phyllites of the Beloretzk Terrane (ACTS'96 transect) provide K-Ar values between 506 (13) Ma in the high-grade metamorphic complex of Beloretzk (MCB) and 737 (24) Ma in the adjacent low-grade metamorphic part of the Beloretzk Terrane. A less pronounced cleavage and a coarser grain size characterize the phyllite with highest K-Ar data. The changes to narrow spaced cleavage domains, less amount of microlithons and smaller grain size are connected to decreasing K-Ar data. Considering the grain size and secondary foliation, the K-Ar dates may indicate an incomplete resetting of a pre-Late Neoproterozoic metamorphic age by a changing ratio between cleavage domains and microlithons caused by the Neoproterozoic orogeny and to a lesser extent by the Uralian orogeny (Glasmacher et al. 2001a). The MCB is characterized by a complex pre-Late Neoproterozoic deformational and metamorphic history (Fig. 11). Glasmacher et al. (2001a) described three pre-Ordovician deformations. The oldest ( $D_1$ ) is Grenvillian in age and is younger than the intrusion of mafic dikes ( $\sim 1,350$  Ma) and older than the eclogite-facies metamorphism. The high P/low T eclogite-facies metamorphism is bracketed by  $D_1$  and the intrusion of the Achmerovo granite (about 970 Ma). The youngest pre-Ordovician deformation indicated by E-vergent folding and thrusting occurred at retrograde greenschist-facies metamorphic conditions and is related to the Late Neoproterozoic orogeny at about 550 Ma (Glasmacher et al. 1999, 2001a). A tremolite  $^{40}\text{Ar}/^{39}\text{Ar}$  cooling age at 718 (5) Ma of amphibolitic-eclogite and muscovite  $^{40}\text{Ar}/^{39}\text{Ar}$  cooling age of about 550 Ma of a micaschist indicate that a temperature of 500 (50) °C, was not reached during the Late Neoproterozoic orogeny. In comparison, the new K-Ar dates of the Beloretzk Terrane indicate that its low-grade metamorphic part reached its peak metamorphic conditions in pre-Late Neoproterozoic time or before 737 (24) Ma. Strong internal deformation during the Late Neoproterozoic orogeny leads to a resetting of the old K-Ar ages. Furthermore, the interpretation of the K-Ar data pattern of the Yamantau anticlinorium indicates that the lower greenschist-facies metamorphism is of pre-Late Neoproterozoic origin or older than 924 (21) Ma. This metamorphism is not related to a deformation. Only one internal deformation occurs in the central part of the Yamantau anticlinorium. The interpretation of the K-Ar data suggests that the deformation is of Late Neoproterozoic age. Glasmacher et al. (2001a) argued, on the basis of geochronological and thermochronological data together with the abrupt change in structural style and metamorphism in the east of the Zuratkul Fault, that the MCB is exotic with respect to the SE-margin of the East European Platform.



The geological process that led to the metamorphism of the Lower Riphean in the central Yamantau anticlinorium is unknown. A pre-Late Neoproterozoic metamorphic age of more than 924 (21) Ma might connect the metamorphic process to the evolution of the Kaltasy aulacogen (Fig. 2). Several deep aulacogens developed in the Archaean crystalline basement at the eastern margin of the EEC and were filled with up to 15 km of Riphean sediments (Peterson and Clarke 1983; Nalivkin and Jacobson 1985; Maslov et al. 1997). In the southern Urals, the Kaltasy aulacogen is important in Riphean time. The sedimentation rate in the Kaltasy aulacogen changed in the late Middle Riphean to early Upper Riphean (Lobkovsky et al. 1996; Maslov et al. 1997). The first occurrence of nearshore and distinctive tidal-flat and shallow-marine deposits is known from top of the Zilmerdak sequence (~970 Ma, Maslov et al. 1997). The sedimentation rate decreased and remained low up to the Vendian (~620 Ma). During the Katav formation (~940 Ma), shallow-marine carbonate sediments were deposited. The total thickness of Riphean sediments overlaying the Lower Riphean units in the Yamantau anticlinorium could have reached up to 14,000 m in the early Upper Riphean (Katav). Assuming a metamorphic temperature of more than 300 °C, a low geothermal gradient of about 21 °C/km would lead to a lower greenschist-facies grade for the burial metamorphism. Furthermore, if the geothermal gradient is the same throughout the Upper Riphean and Vendian, the K-Ar age of 924 (21) Ma implies that the thickness of the Upper Riphean sediments in the Yamantau anticlinorium could have been thin and that the Yamantau anticlinorium was not covered by Vendian sedimentary deposits. The upper part of the Middle Riphean has reached an upper anchizone metamorphic grade at the western limb of the Yamantau anticlinorium. This implies that the age of incipient metamorphism cannot be Upper Riphean. According to Merriman and Frey (1999), the temperature range for the anchizone is between about 200 and 300 °C, whereas Mullis et al. (2002) shifted the lower side of the temperature range to 240 (15) °C. Considering a temperature of more than 260 °C and a maximum thickness of about 9,000 m of Upper Riphean and Vendian sediments, a geothermal gradient of about 29 °C/km would be necessary to increase the Kübler index to upper anchizone values at the end of the Vendian (540 Ma). If the incipient metamorphism at the western limb of the Yamantau anticlinorium is of Vendian age, the S1 cleavage has only partly reset detrital K-Ar ages. According to Hunziker et al. (1986), a temperature of 260 (30) °C is necessary to release the

whole radiogenic  $^{40}\text{Ar}$  out of  $<2\ \mu\text{m}$  illite particles. The youngest K-Ar data at the western limb of the Yamantau anticlinorium might, therefore, represent the age of metamorphism and the development of the S1 cleavage (Fig. 11). Further to the west in the Ala-Tau anticlinorium, Glasmacher et al. (1999, 2001a) described a Late Neoproterozoic to Early Cambrian resetting of microcline  $^{40}\text{Ar}/^{39}\text{Ar}$  ages in Vendian and Upper Riphean conglomerates (Fig. 11). The microcline is partly embedded in granite pebbles. Orthoclase from the granite pebbles yielded  $^{40}\text{Ar}/^{39}\text{Ar}$  spectra of about 600–640 Ma. Muscovite from one of the granite pebbles is characterized by a well-defined  $^{40}\text{Ar}/^{39}\text{Ar}$  plateau age at 699 (3) Ma. The K-Ar data, together with regional geological, suggest that the central part of the Yamantau anticlinorium located east of the main Avzyan thrust, was metamorphosed in Upper Riphean times. West of the main Avzyan thrust, including an area from the western limb of the Yamantau anticlinorium to the western part of the Ala-Tau anticlinorium, the Middle Riphean to Vendian sediments were metamorphosed during the Late Neoproterozoic orogeny. This orogeny also partly reset the pre-Late Neoproterozoic illite ages in the eastern Yamantau anticlinorium and the Beloretzk Terrane (Fig. 11).

## Conclusion

The available geochronological results give evidence for a complex pre-Uralian metamorphic history and deformation of the Precambrian basement at the southeastern margin of the East European Craton. In addition, more circumstantial evidence exists for an early Neoproterozoic metamorphism in the central and eastern Yamantau anticlinorium. The following conclusions are derived from the study of the foliation, the Kübler and Árkai Index values, and the K-Ar dates of the  $<2$ ,  $<0.8$  and  $0.2\text{-}\mu\text{m}$ -size fractions of phyllites and slates:

1. The central and eastern part of the Yamantau anticlinorium, to the East of the main Avzyan thrust, was metamorphosed to lower greenschist-facies grade in early Neoproterozoic times (Upper Riphean, ~970 Ma). No indications were found for deformation during the burial metamorphism.
2. To the west of the main Avzyan thrust diagenetic to incipient metamorphic grade was reached in Late Neoproterozoic times. Late Neoproterozoic (~540 Ma) internal deformation developed up to the westernmost Avzyan thrust.
3. Uralian internal deformation and resetting of older K-Ar ages are restricted to thrusts and faults in the Bashkirian Mega-anticlinorium
4. The Proterozoic K-Ar ages were stronger reset by the Uralian deformation in the footwall of the Palaeozoic nappe stack, which originated during the Uralian deformation. The influence of the Uralian internal deformation, the latter caused by the nappe emplacement on top of the Riphean siliciclastic rocks at the surface,

**Fig. 11** t-T-D path of the metamorphic complex of Beloretzk (MCB, Glasmacher et al. 2001a), the Yamantau and the Ala-Tau anticlinorium (2  $\sigma$ -error quoted), LV Lower Vendian, UV Upper Vendian, time scale adapted from Kozlov et al. (1995); international time-scale after Haq and Eysinga 1998. (References to Pb-Pb zircon ages, K-Ar feldspar ages as well as  $^{40}\text{Ar}/^{39}\text{Ar}$  ages on amphibole, muscovite and microcline are Glasmacher et al. 1999, 2001a)

- decreases with increasing distance and therefore reached not very far into the Precambrian basement of the East European Craton.
5. Similarly to the high-grade metamorphic part of the Beloretzk Terrane, the adjacent area of greenschist-facies grade was metamorphosed before the Late Neoproterozoic orogeny
  6. The Late Neoproterozoic orogeny induced the dominant S1 cleavage in the area of greenschist-facies grade in the Beloretzk Terrane
  7. The post-Uralian erosion has not yet reached rocks with a cleavage of Uralian age. Late Neoproterozoic thrusts and faults at the eastern margin of the East European Craton have been reactivated during the Uralian deformation

**Acknowledgments** Fieldwork in the Ural and laboratory studies were funded by the Deutsche Forschungsgemeinschaft (DFG) grants Gl 182/3-1, /3-2, /3-3, /3-4, which are gratefully acknowledged. This paper is a contribution to EUROPROBE (URALIDES). EUROPROBE is co-ordinated within the International Lithosphere Program and is sponsored by the European Science Foundation. As a representative of the Russian team during the fieldwork, we thank Dr. V. N. Baryshev for his scientific and logistical help. Special thanks are given to Prof. R. Walter, Drs. U. Giese, L. Stroink and I. Matenaar for their help and support during fieldwork and many fruitful discussions. Furthermore, the authors like to thank Prof. Eynatten, Prof. Massonne, Drs. Merriman and Árkai, and an unknown reviewer for their helpful suggestions on earlier versions of the manuscript. We acknowledge the technical assistance of R. Wendling and T. Peyrone (Centre de Géochimie de la Surface, CNRS/ULP). This is EOST contribution no. AAA.NNN-UMR7517x.

## References

- Alekseyev AA (1984) Riphean and Vendian magmatism in the southern Urals [in Russian]. Nauka, Moscow, pp 1–136
- Alekseyev AA, Alekseyeva GV (1988) Magmatism, metamorphism and palaeotectonic of the Late Precambrian at the western slope of the Uralides. In: The Upper Precambrian of the southern Urals and the eastern part of the Russian platform [in Russian]. Bashkirskii Nauch. Tsentr Uralskogo, pp 54–59
- Árkai P (1991) Chlorite crystallinity: an empirical approach and correlation with illite crystallinity, coal rank and mineral facies as exemplified by Palaeozoic and Mesozoic rocks of northeast Hungary. *J Metamorph Geol* 9:723–734
- Árkai P, Sassi FP, Sassi R (1995) Simultaneous measurements of chlorite and illite crystallinity: a more reliable tool for monitoring low- to very low grade metamorphism in metapelites. A case study from the Southern Alps (NE Italy). *Eur J Mineral* 7:1115–1128
- Árkai P, Merriman RJ, Roberts B, Peacor DR, Tóth M (1996) Crystallinity, crystallite size and lattice strain of illite-muscovite and chlorite: comparison of XRD and TEM data for diagenetic and epizonal pelites. *Eur J Mineral* 8:1119–1137
- Árkai P, Balogh K, Frey M (1997) The effects of tectonic strain on crystallinity, apparent mean crystallite size and lattice strain of phyllosilicates in low-temperature metamorphic rocks: a case study from the Glarus overthrust, Switzerland. *Schweiz Mineral Petrograph Mitteil* 77:27–40
- Árkai P, Ferreira Máhlmann R, Suchý V, Balogh K, Sýkorová J, Frey M (2002) Possible effects of tectonic shear strain on phyllosilicates: a case study from the Kandersteg area, Helvetic domain, Central Alps, Switzerland. *Schweiz Mineral Petrograph Mitteil* 82:273–291
- Bastida F, Aller J, Puchkov VN, Juhlin C, Oslianski A (1997) A cross-section through the Zilair Nappe (southern Urals). *Tectonophysics* 276:253–264
- Bonhomme M, Thuizat R, Pinault Y, Clauer N, Wendling R, Winkler R. (1975) Méthode de datation Potassium-Argon: appareillage et technique. Note technique. no. 3, Institut Géologique, Université Louis-Pasteur, Strasbourg
- Bons A-J (1988) Intracrystalline deformation and slaty cleavage development in very low-grade slates from the Central Pyrénées. *Geol Ultraiect* 56: 1–173
- Borradaile GJ, Bayly MB, Pwell CMA (1982) Atlas of deformational and metamorphic rock fabrics. Springer, Berlin Heidelberg New York
- Brix MR, Stöckhert B, Seidel E, Theye T, Thomson SN, Küster M (2002) Thermobarometric data from a fossil zircon partial annealing zone in high pressure–low temperature rocks of eastern and central Crete, Greece. *Tectonophysics* 349:309–326
- Brown D, Puchkov V, Alvarez-Marron J, Perez-Estaun A (1996) The structural architecture of the footwall to the Main Uralian Fault, southern Urals. *Earth Sci Rev* 40:125–147
- Brown D, Juhlin C, Alvarez-Marron J, Perez-Estaun A, Oslianski A (1998) Crustal-scale structure and evolution of an arc-continent collision zone in the southern Urals, Russia. *Tectonics* 17:158–171
- Clauer N (1974) Utilisation de la méthode rubidium-strontium pour la datation d'une schistosité de sédiments peu métamorphisés: Application au Précambrien II de la boutonnière de Bou Azzer-El Graara (Anti-Atlas). *Earth Planet Sci Lett* 22:404–412
- Clauer N, Chaudhuri S (1995) Clays in crustal environments: isotope dating and tracing. Springer, Berlin Heidelberg New York, 359 pp
- Clauer N, Chaudhuri S (1998) Isotopic dating of very low-grade metasedimentary and metavolcanic rocks: techniques and methods. In: Frey M, Robinson D (eds) Low-grade metamorphism. Blackwell, Oxford, pp 202–226
- Clauer N, Rais N, Schaltegger U, Piqué A (1995) K-Ar systematics of clay-to-mica minerals in a multi-stage low-grade metamorphic evolution. *Chem Geol* 124:305–316
- Clauer N, Weber F, Gauthier-Lafaye F, Toulkeridis T, Sizun JP (1997) Mineralogical, geochemical (REE), and isotopic (K-Ar, Rb-Sr, <sup>18</sup>O) evolution of the clay minerals from faulted, carbonate-rich, passive paleomargin of the Southeastern Massif Central, France. *J Sedimentol Res* 67:923–934
- Frank B (1987) Bestimmung des Metamorphosegrades der paläozoischen Schichten des Venn-Großsattels (Linksrheinisches Schiefergebirge) mit Hilfe der Illit-Kristallinität und Untersuchung der Zusammenhänge zwischen dem Metamorphosegrad und den regionalen tektonischen Verhältnissen. Doktorarbeit, Rheinisch Westfälische Technische Hochschule, Aachen, pp 1–206
- Fernández-Caliani J, Galan E (1992) Influence of tectonic factors on illite crystallinity: a case study in the Iberian Pyrite belt. *Clay Minerals* 27:385–388
- Gafarov RA (1970) On the deep structure of the basement in the conjugation zone between the East-European platform and the Urals [in Russian]. *Izvestiya* 8(N):3–14
- Garris MA (1977) The stages of magmatism and metamorphism in the pre-Jurassic history of the Urals and Cis-Urals. Naukala, Moscow, 295 pp
- Garver JI, Bartholomew A (2001) Partial resetting of fission tracks in detrital zircon: dating low temperature events in the Hudson Valley (NY). *GSA Spec Pap* 33:83
- Gee DG, Zeyen HJ (1996) Lithosphere dynamics: origin and evolution of continents. Secretary EUROPROBE 1996, Uppsala University, Uppsala, Sweden
- Getsen VG, Dedeev VA, Akimova GN, Andreichev VL, Bashilov VI, Belyakova LT, Gornostay BA, Dembovsky BY (1987) The Riphean and Vendian of the European North of the USSR [in Russian]. Komi Filial AN SSSR, Institute of Geology, Syktyvkar
- Giese U, Glasmacher UA, Kozlov V, Matenaar I, Puchkov V, Stroink L, Bauer W, Ladage S, Walter R (1999) Structural

- framework of the Bashkirian Anticlinorium, SW Urals. *Geol Rundsch* 87:526–544
- Glasmacher U, Matenaar I, Pickel W, Giese U, Kozlov VI, Puchkov V, Stroink L, Walter R (1997) Incipient metamorphism of the western fold-and-thrust belt, Southern Urals, Russia. *Beih Z Eur J Mineral* 9:124
- Glasmacher UA, Reynolds P, Alekseev A, Puchkov V, Taylor K, Gorozhanin V, Walter R (1999)  $^{40}\text{Ar}/^{39}\text{Ar}$  Thermochronology west of the main Uralian Fault, Southern Urals, Russia. *Geol Rundsch* 87:515–525
- Glasmacher UA, Bauer W, Giese U, Reynolds P, Kober B, Puchkov VN, Stroink L, Alekseev A, Willner A (2001a) The metamorphic complex of Beloretzk, SW Urals, Russia: a terrane with a polyphase Meso- to Neoproterozoic thermo-dynamic evolution. *Precambrian Res* 110:185–213
- Glasmacher UA, Tschernoster R, Clauer N, Spaeth G (2001b) K-Ar dating of magmatic sericite crystallites for determination of cooling paths of metamorphic overprints. *Chem Geol* 175:673–687
- Glasmacher UA, Wagner GA, Puchkov VN (2002) Thermo-tectonic evolution of the western fold-and-thrust belt, Southern Urals, Russia, as revealed by apatite fission-track data. *Tectonophysics* 354:25–48
- Glasmacher UA, Matenaar I, Bauer W, Puchkov VN (2004) Diagenesis and incipient metamorphism in the western fold-and-thrust belt, SW Urals, Russia. *Int J Earth Sci* 93: 361–383
- Goldin BA, Fishman MV, Kalinin YeP, Davydov VA (1973) Volcanic complexes in the North of the Urals [in Russian]. Nauka, Leningrad
- Gorbatshev R, Bogdanova S (1993) Frontiers in the Baltic Shield. *Precambrian Res* 64:3–21
- Gorokhov IM, Semikhatov MA, Baskakov AV (1995) Isotopic composition of strontium in carbonate rocks of the Riphean, Vendian and Lower Cambrian of Siberia. *Stratigr Geol Correl* 3:3–33
- Gorozhanin VM (1990) Geochronology of the Lower Vendian of the Southern Urals. In: *The stratigraphy of the Upper Proterozoic of the USSR (Riphean and Vendian)* [in Russian]. Bashkirian Science Centre, Ufa, pp 51–52
- Gorozhanin VM (1995) Rubidium-strontium isotope method in solving of problems of the Southern Urals [in Russian]. Referat of the Candidate Thesis, Institute of Geology and Geochemistry, Ekaterinburg, 23 pp
- Guggenheim S, Bain DC, Bergaya F, Brigatti MF, Drits VA, Eberl DD, Formoso MLL, Galán E, Merriman RJ, Peacor DR, Stanjek H, Watanabe T (2002) Report of the association internationale pour L'Étude des argyles (AIPEA) nomenclature committee for 2001: Order, disorder and crystallinity in phyllosilicates and the use of the "Crystallinity index". *Clays Clay Miner* 50:406–409
- Haq BU, Eysinga van FWB (1998) *Geological time table*, 5th edn. Elsevier, Amsterdam
- Hasebe N, Mori S, Tagami T, Matsui R (2003) Geological partial annealing zone of zircon fission-track system: additional constraints from the deep drilling MITI-Nishikubiki and MITI-Mishima. *Chem Geol* 199:45–52
- Hunziker JC, Frey M, Clauer N, Dallmeyer RD, Friedrichsen H, Flehmig W, Hochstrasser K, Roggwiler P, Schwander H (1986) The evolution of illite to muscovite: mineralogical and isotopic data from the Glarus Alps, Switzerland. *Contrib Mineral Petrol* 92:157–180
- Huon S, Piqué A, Clauer N (1987) Etude de l'orogénèse hercynienne au Maroc par la datation K-Ar de l'évolution métamorphique de schistes ardoisiers. *Sci Géol Bull* 40:273–284
- Huon S, Cornée JJ, Piqué A, Rais N, Clauer N, Liewig N, Zayane R (1993) Mise en évidence au Maroc d'évènements thermique d'âge triasico-liasique liés à l'ouverture de l'Atlantique. *Soc Géol Fr* 164:165–176
- Ivanov SN (1987) On the Baykalides of the Urals and nature of metamorphic complexes flanking eugeosynclines [in Russian]. Institute of Geology and Geochemistry, Sverdlovsk
- Jaboyedoff M, Cosca MA (1999) Dating incipient metamorphism using  $^{40}\text{Ar}/^{39}\text{Ar}$  geochronology and XRD modelling: a case study from the Swiss Alps. *Contrib Mineral Petrol* 135:93–113
- Kasuya HG, Naeser CW (1988) The effect of  $\alpha$ -damage of fission-track annealing in zircon. *Nucl Tracks Radiat Measure* 14:477–480
- Kheraskov NP (1967) *Tectonica and formations* [in Russian]. Izbrannye trudy Nauka, Moscow
- Kisch HJ (1991) Illite crystallinity: recommendations on sample preparation, X-ray diffraction settings, and interlaboratory samples. *J Metamorph Geol* 9:665–670
- Kligfield R, Hunziker J, Dallmeyer RD, Schamel S (1986) Dating of deformation phases using the K-Ar and  $^{40}\text{Ar}/^{39}\text{Ar}$  techniques: results from the Northern Apennines. *J Struct Geol* 8:781–798
- Kozlov VI (1982) Upper Riphean and Vendian in the Southern Urals [in Russian]. Nauka, Moscow, pp 1–128
- Kozlov VI, Krasnobaev AA, Larionov NN, Maslov AV, Sergeeva ND, Ronkin YuL, Bibikova EV (1989) Lower Riphean of the southern Urals [in Russian]. Nauka, Moscow, 208 pp
- Kozlov VI, Sinitsyna ZA, Kulagina EI, Pazukhin VN, Puchkov VN, Kochetkova NM, Abramova AN, Klimenko TV, Sergeeva ND (1995) Guidebook of excursion for the Palaeozoic and Upper Precambrian sections of the western slope of the Southern Urals and Preuralian regions. Ufa Science Center, RAS, Ufa, 165 pp
- Kralik M (1983) Interpretation of K-Ar and Rb-Sr data from fine fractions of weakly metamorphosed shales and carbonate rocks at the base of the Northern Calcareous Alps (Salzburg, Austria). *Tschermaks Minera Petrol Mitteil* 32:49–67
- Krasnobaev AA (1986) Zircon as an indicator of geological processes [in Russian]. Nauka, Moscow, 145 pp
- Krumm S, Buggisch W (1991) Sample preparation effects on illite crystallinity measurement: grain-size gradation and particle orientation. *J Metamorph Geol* 9:671–677
- Leitch EC, McDougall I (1979) The age of orogenesis in the Nambucca Slate belt: A K-Ar study of low-grade regional metamorphic rocks. *J Geol S Aust* 26:111–119
- Lobkovsky LI, Cloetingh S, Nikishin AM, Volozh YuA, Lankreijer AC, Belyakov SL, Groshev VG, Fokin PA, Milanovsky EE, Pevzner LA, Gorbachev VI, Korneev MA (1996) Extensional basins of the former Soviet Union: structure, basin formation mechanisms and subsidence history. *Tectonophysics* 266:251–285
- Maslov AV, Erdtmann BD, Ivanov KS, Ivanov SN, Krupenin MT (1997) The main tectonic events, depositional history, and the paleogeography of the Southern Urals during the Riphean-Early Palaeozoic. *Tectonophysics* 276(1–4):313–335
- Maslov AV, Krupenin MT, Gareev EZ, Anfimov LV (2001) The Riphean of the western slope of the Southern Urals, vol 1. Zavarit. Inst. Geol., Ekaterinburg, 351 pp
- Matenaar I, Glasmacher UA, Pickel W, Giese U, Pazukhin VN, Kozlov VI, Puchkov VN, Stroink L, Walter R (1999) Incipient metamorphism between Ufa and Beloretzk, western fold-and-thrust belt, Southern Urals, Russia. *Geol Rundsch* 87:545–560
- Merriman RJ, Frey M (1999) Patterns of very low-grade metamorphism in metapelitic rocks. In: Frey M, Robinson D (eds) *Low-grade metamorphism*. Blackwell, Oxford, pp 61–107
- Merriman RJ, Peacor DR (1999) Very low-grade metapelites: mineralogy, microfabrics and measuring reaction progress. In: Frey M, Robinson D (eds) *Low-grade metamorphism*. Blackwell, Oxford, pp 10–60
- Merriman RJ, Roberts B, Peacor DR, Hiron SR (1995) Strain-related differences in the crystal growth of white mica and chlorite: a TEM and XRD study of the development of metapelites microfabrics in the Southern Uplands thrust terrane, Scotland. *J Metamorph Geol* 13:559–576
- Mullis J, Rahn MK, Schwer P, de Capitani C, Stern WB, Frey M (2002) Correlation of fluid inclusion temperatures with illite "crystallinity" data and clay mineral chemistry in sedimentary rocks from the external part of the Central Alps. *Schweiz Mineral Petrogr Mitteil* 82:325–340

- Murrell GR (2003) The long-term thermal evolution of Central Fennoscandia revealed by low-temperature thermochronology. PhD Thesis, Vrije Universiteit, Amsterdam, 219 pp
- Nalivkin V, Yacobson K (1985) Russian platform [in Russian]. Nedra, Leningrad, 356 pp
- Nikishin V, Ziegler PA, Stephenson RA, Cloetingh SAPL, Furne AV, Fokin PA, Ershov AV, Bolotov SN, Korotaev MV, Alekseev AS, Gorbachev VI, Shipilov EV, Lankreijer A, Bembinova EY, Shalimov IV (1996) Late Precambrian to Triassic history of the East European Craton: dynamics of sedimentary basin evolution. *Tectonophysics* 268:23–63
- Nikishin V, Furne AV, Ziegler P (1997) Riphean–Vendian geological history and geodynamics of the East European Craton. *Moscow Univ Geol Bull* 52:9–20
- Nyk R (1985) Illite crystallinity in Devonian slates of the Meggen mine (Rhenish Massif). *Neues Jahrb Miner Monatsh* 268–276
- Ovchinnikova GV, Gorokhov IM (2000) Pb–Pb dating of carbonate sedimentary rocks of the Upper Proterozoic [in Russian]. In: Problems of the lithology, geochemistry and ore genesis of the sedimentary process. Abstr. of the 12th All-Russian Lithological Meeting 2, Moscow, pp 84–88
- Ovchinnikova GV, Gorokhov IM, Semikhatov MA (1995) The time of formation and transformation of the deposits of the Inzer svita, Upper Riphean of the Southern Urals: general problems of the stratigraphy and geological history of the Riphean of northern Eurasia [in Russian]. *Uralian Branch of RAS, Ekaterinburg*, pp 73–75
- Ovchinnikova GV, Vasilieva IM, Semikhatov MA (1998) U–Pb systematics of Proterozoic carbonate rocks: Inzer svita of the Upper Riphean (Southern Urals) [in Russian]. *Stratigr Geol Correl* 6:20–31
- Parnachev VP (1981) Volcanic complexes and tectonic regime of the western slope of the Urals in the Late Precambrian [in Russian]. In: Ancient volcanism of the Southern Urals. Ufimian Scientific Centre, Ufa, pp 18–30
- Parnachev VP, Kozlov VI, Titunina IV (1981) New data on the structure, composition and origin of the Arsha metavolcanic complex of the Southern Urals (Late Precambrian) [in Russian]. *Sverdlovsk*, pp 69–86
- Passchier CW, Trouw RAJ (1996) *Microtectonics*. Springer, Berlin Heidelberg New York, 289 pp
- Peterson JA, Clarke JW (1983) Petroleum geology and resources of the Volga-Ural Province, USSR. USGS Circular 885, USGS, Reston, Virginia, 27 pp
- Powell CM (1979) A morphological classification of rock cleavage. *Tectonophysics* 58:21–34
- Puchkov VN (1997) Structure and geodynamics of the Uralian orogen. In: Burg JP, Ford M (eds) *Orogeny through time*. *Geol Soc London Spec Publ* 121:201–236
- Puchkov VN (2000) Palaeogeodynamics of the Central and Southern Urals. *Pauria*, Ufa, pp 1–145
- Rahn MKW (2001) The metamorphic and exhumation history of the Helvetic Alps, Switzerland, as revealed by apatite and zircon fission tracks. PhD Thesis, Universität Freiburg, Freiburg, 140 pp
- Reuter A (1987) Implications of K–Ar ages of whole-rock and grain-size fractions of metapelites and intercalated metatuffs within an anchizonal terrane. *Contrib Mineral Petrol* 97:105–115
- Riley BCD (2002) Preferential thermal resetting of fission tracks in radiation-damaged detrital zircon grains: case study from the Laramide of Arizona. GSA Paper no. 212-12, GSA, Boulder, Colorado
- Roberts B, Merriman RJ (1985) The distinction between Caledonian burial and regional metamorphism in metapelites from north Wales: an analysis of isocryst patterns. *J Geol Soc* 142:615–624
- Roberts D, Siedlecka A (2002) Timanian orogenic deformation along the northeastern margin of Baltica, northwest Russia and northeast Norway, and Avalonia–Cadomian connections. *Tectonophysics* 352:169–184
- Romanov VA, Isherskaya MV (1994) On the Riphean series of the Western Bashkiria [in Russian]. Institute of Geology, Ufa
- Schaltegger U, Stille P, Rais N, Piqué A, Clauer N (1994) Neodymium and strontium isotopic dating of diagenesis and low-grade metamorphism of argillaceous sediments. *Geochim Cosmochim Acta* 58:1471–1481
- Semikhatov MA, Shurkin KA, Aksenov EM (1991) A new Precambrian stratigraphic scale in the USSR. *Isv AN USSR Ser geol* 4:3–13
- Seward D, Pérez-Estaún A, Puchkov VN (1997) Preliminary fission-track results from the Southern Urals: Sterlitamak to Magnitogorsk. *Tectonophysics* 276:281–290
- Sobolev AE (1996) Middle Riphean basic dikes in the Yamantau Anticlinorium. *Doklady Earth Sci* 359(A):356–359
- Steiger RH, Jäger E (1977) Subcommittee on geochronology: convention on the use of decay constants in geo- and cosmochronology. *Earth Planet Sci Lett* 36:359–362
- Stroink L, Frese K, Giese U, Matenaar I, Kozlov VI, Glasmacher U, Puchkov V, Walter R (1997) Compositional framework of Upper Proterozoic sandstones of the Southern Urals: implications for a Pre-Uralian orogenic event. 18th IAS, Heidelberg, p 324
- Tagami T, Shimada C (1996) Natural long-term annealing of zircon fission track system around a granitic pluton. *J Geophys Res* 101(B):11353–11364
- Tagami T, Galbraith RF, Yamanda R, Laslett GM (1998) Revised annealing kinetics of fission tracks in zircon and geological implications. In: Van den haute P, De Corte F, (eds) *Advances in fission-track geochronology*. Kluwer, Dordrecht, pp 99–112
- Toulkeridis T, Goldstein SL, Clauer N, Kröner A, Lowe DR (1994) Sm–Nd dating of fig tree clay minerals of the Barberton Greenstone Belt. *South African Geol* 22:199–202
- Wang H, Frey M, Stern WB (1996) Diagenesis and metamorphism of clay minerals in the Helvetic alps of Eastern Switzerland. *Clays Clay Miner* 44:96–112
- Warr LN, Rice AHN (1994) Interlaboratory standardization and calibration of clay mineral crystallinity and crystallite size data. *J Metamorph Geol* 12:141–152
- Willner AP, Emolaeva T, Stroink L, Glasmacher UA, Giese U, Puchkov V, Kozlov VI, Walter R (2001) Contrasting provenance signals in Riphean and Vendian sandstones in the SW Urals (Russia): constraints for a change from passive to active continental margin conditions in the Neoproterozoic. *Precambrian Res* 110:215–239
- Willner AP, Sindern S, Metzger R, Emolaeva T, Kramm U, Puchkov V, Kronz A (2003) Typology and single grain U/Pb ages of detrital zircons from Proterozoic sandstones in the SW Urals (Russia): early time marks at the eastern margin of Baltica. *Precambrian Res* 124:1–20
- Yamada R, Tagami T, Nishimura S, Ito H (1995) Annealing kinetics of fission tracks in zircon: an experimental study. *Chem Geol* 122:249–258
- Zaitseva TS, Ivanovskaya TA, Gorokhov IM (2000) Rb–Sr age and NR-spectres of glauconites of the Uk svita, Upper Riphean Southern Urals. In: *Isotopic dating of geological processes: new method and its results* [in Russian]. GEOS, Moscow, pp 144–147
- Zhao MW, Ahrendt H, Wemmer K (1997) K–Ar systematics of illite/smectite in argillaceous rocks from the Ordos basin, China. *Chem Geol* 136:153–169
- Zhao B, Clauer N, Robb LJ, Zwingmann H, Toulkeridis T, Meyer FM (1999) K–Ar dating of white micas from the Ventersdorp contact reef of the Witwatersrand Basin, South Africa: timing of post-depositional alteration. *Mineral Petrol* 66:149–170